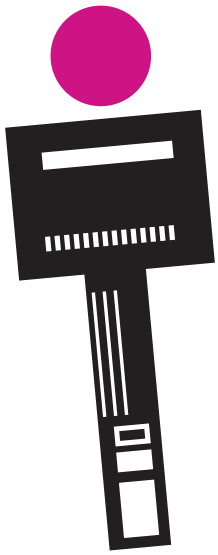

RAM ROBOTICS AND MECHATRONICS

DEVELOPING A RELIABLE METHOD TO CONNECT CONDUCTORS TO 3D PRINTED CONDUCTING STRUCTURES

P. (Patrick) Neuvel

BSC ASSIGNMENT

Committee:
prof. dr. ir. G.J. M. Krijnen
ir. A.P. Dijkshoorn
dr. ir. W. Olthuis

August, 2020

028RaM2020
Robotics and Mechatronics
EEMathCS
University of Twente
P.O. Box 217
7500 AE Enschede
The Netherlands

UNIVERSITY OF TWENTE. | TECHMED CENTRE UNIVERSITY OF TWENTE. | DIGITAL SOCIETY INSTITUTE

Abstract

3D-printed sensors are a novel but foremost complicated matter, for using these 3D-Printed sensors in practical applications they have to be connected to a metal conductor. This report Will dive into the details of how such a connection between conductive polymer and metal can be created and, foremost important be made mechanically and electrically reliable.

Perforated copper tape with lots of 600 µm holes, overmolded by a 3D-printer's nozzle, performed from all the tested methods in this report by far the best. By this is meant in terms of mechanical strength and electrical stability. For the overmolding to be successful, the bed temperature of the sample is set to at least 65°C. This will let the sample warm-up and will prevent the conductive polymer extruded out of the nozzle, from cooling to fast and make an insufficiently weak bond through the holes of the perforated tape.

Furthermore, This report will also introduce a new method, the In-Situ resistance measurement. This method means that the conductive samples are monitored from the moment that the printer starts printing. This method revealed that an extrusion multiplier above 100% (110%, 120%) resulted in a sample with increased internal resistance, which stayed permanent even after settling for several days. Compared to a sample printed with a multiplier of 100%.

Acknowledgements

I would like to tank my parents for supporting me throughout my life and making it possible to have such a sophisticated lab at home, which let me do physical experiments even when the university is closed during a pandemic. Furthermore, I would like to give a big overall thank you, to my committee: Alexander Dijkshoorn, Gijs Krijnen, and Wouter Olthuis. Now the personal acknowledgements: Thank you Alexander for helping me on a daily and nightly basis (less sleep more research kinda motto :p) and supplying me with the supplies needed for this research. Thankyou Gijs Krijnen for, offering many ideas but in particular the one of making holes in the copper tape with a steel brush, which turned out to be key advice for this research. And last but surely not least, thank you Wouter Olthuis for your time and feedback during the midterm presentation and to make the committee complete!

Contents

1 Introduction

3D printing with conductive polymers (filaments) is a complicated matter, the individual traxels (which are short for 3D printed tracks by the nozzle) that make up a sensor, form a complicated network [1]. In this network, conduction will take place. This 3D printed conducting network needs to be connected to a conductor e.g. a wire or copper tape to give it a practical application. To the day of this report's publication, there isn't a known and tested standard to connect a 3D printed sensor made of conducting polymer to a conductor. Figure 1.1 show two methods commonly used by RaM [2] for connecting their conductors to a 3D printed sensor. Extending the two types of contacts shown in Figure 1.1 with an additional paper [5], a few

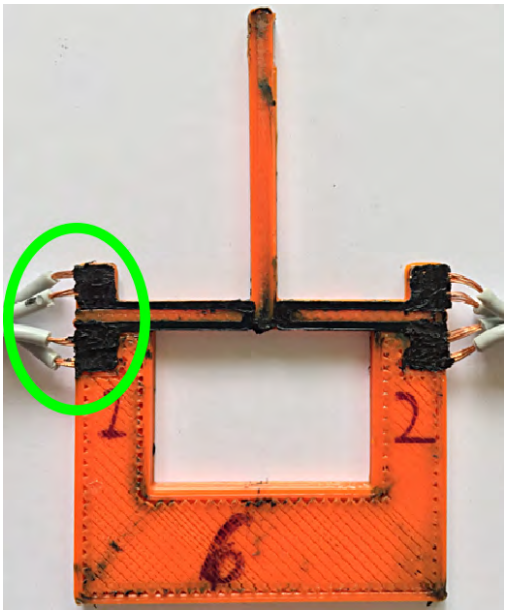

(a) Using a soldering iron to melt-in conductive wires into the conductive filament to establish a connection (green circle) [3]

(b) Using copper tape combined with silver paint to establish a connection between the conductive filament and the conductor [4]

Figure 1.1: Two different methods to connect a conductor to a piece of 3D printed filament

more techniques are presented, these techniques are: friction fitting a barrel and spade terminal and a wire, of 1.3 mm in diameter into the 3D printed test piece (Section 3, Figure 3.8). The results of these resistance experiments, together with copper tape and silver paste can be found in section 3 in Table 3.1. Despite so many different connection techniques were tried in these experiments, still, no concrete and tested methods have been found yet. These tried methods do not ensure an electrically predictable and mechanically stable connection. This report will, therefore, dive into the details that could make these yet unpredictable electrical and mechanical properties of a contact predictable and consistent.

Out of the tested concept ideas, did the overmolded perforated copper tape performed the best. However, the measured values of the test samples, using this fabrication method (phase II) did not have the expected low resistance value. Therefore, In-Situ (during print) resistance measurement technique was introduces in order to have a attempt to trace down the source of these unexpected results.

2 Report Structure

This chapter will briefly explain the report structure, the report consist of 5 main chapters listed below: The content of each chapter is briefly discussed.

Literature and experiments by others: In this chapter will literature be presented that explains the basis of a contact between two dissimilar materials. In addition to that, experiments performed by other researchers will be covered. And final, the RaM sensor investigation will be shown, in order to get a grasp of what mechanical and electrical requirements a reliable contact-standard should have.

Phase I - Exploratory research into, conductor and conductive-filament connections: This chapter will explain the first phase of this research, this phase starts with elaborating on the RaM sensor summary and follows with exploratory experiments. Using: PI-ETPU 95-250 (ETPU for short), ProtoPasta conductive PLA (EPLA for short) and copper tape to get familiar with the available materials.

Phase II - Dissimilar material[1] connections by mechanical interlocking: This chapter will explain the second phase of the research, the best setup from phase 1 will be further characterised. This includes mechanical cycle testing and the electrical characterisation paired with these mechanical cycle tests, for ETPU only.

Phase III - In-Situ Resistance Monitoring: This chapter is a branch off of Phase II and tries to investigate some of the unexpected phenomena found in the experiments of Phase II. This by monitoring test sample during printing, the paper covering this new method is added into Appendix A in phase III extra's

Over-all (Rode Draad) Conclusion and Discussion: This is the final chapter and will combine all of the findings from the experiments in Phase I, II, and III and draw a suitable conclusion. This chapter will also contain a discussion about things that could have done better and things that can be done as a follow-up on this research, to further close the gap for achieving predictable and reliable contacts.

(**Note:** *the words polymer and filament mean the same thing in this report*)

[1] So a conductor and a 3D-printed conductive part

3 Literature and experiments by others:

This chapter will cover some models, literature, and experiments performed by others. To get an idea of how metals and conductive polymers (dissimilar materials) can be joined together, mechanically and electrically. Furthermore, will this chapter contain the RaM sensor investigation, this is a table that contains most of the thesis-sensors from RaM graduate students. This table gives a guideline of how large the contact areas have to be and what kind of electrical behaviour is desired for these contacts. A ported version (from Excel) of this table can be seen in Table 3.2 and Table 3.3 the table is split up because it is so large, that it doesn't fit on one page even after condensing and removing some of the columns.

3.1 Asperities and surface roughness

To understand what happens to the mechanical adhesion and electrical conduction when two dissimilar materials touch each other we need to zoom in on the surface of the two touching materials. For a human eye, a material's surface may look smooth, but zooming in on the surface, structures depicted in Figure 3.1 can be seen. These mountain-like structures are

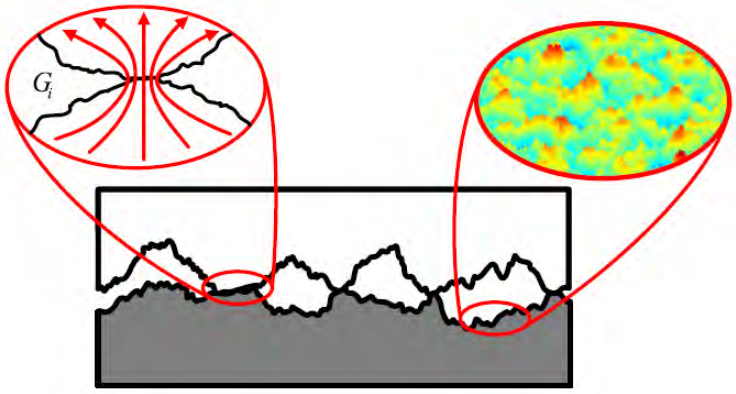

Figure 3.1: The schematic representation of a close up from two surfaces touching each other. [6]

called asperities [6], when two materials are pressed together the asperities on both surfaces can touch each other. On the points were these asperities touch, a current can flow from the bulk of one material to another. The location where this current can flow are called "Holm a-spots" [7], these a-spots will be explained in the next two sections. The current flow from bulk to bulk through a-spot can be seen in the left red circle in Figure 3.1. The asperities mentioned previously can be seen in an SEM picture from a paper that has roughed the surface of aluminium samples with different coarseness of sand blasting. Below the SEM images, a graph is shown, in these graphs the surface height variation can be seen by each surface treatment this can be seen in Figure 3.2

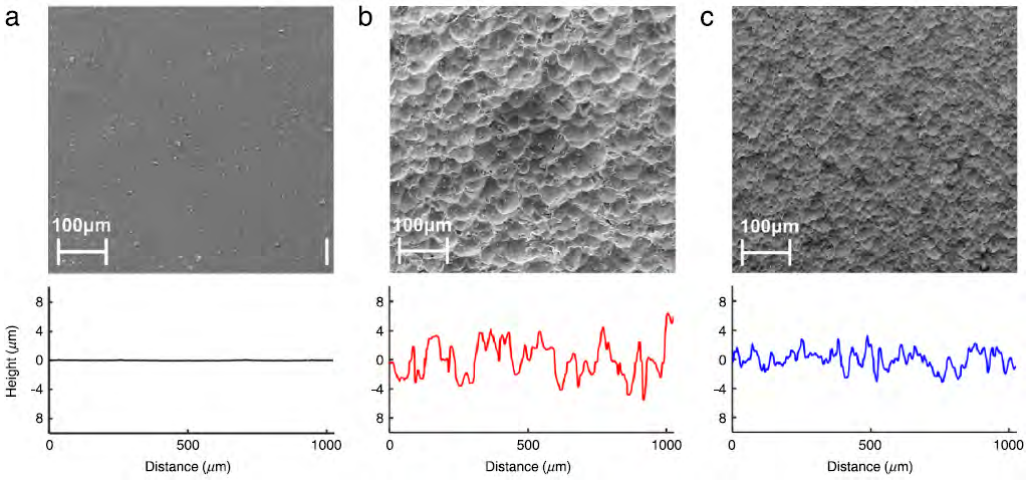

Figure 3.2: SEM images of the surface roughness of aluminium test samples. (a) polished, (b) sand blasted with 300μm beads, (c) sand blasted 50μm [6]

3.2 A-spot in models DC case

The literature in this research will only cover DC (direct current), AC is foremost important as well, but for the experiments used in this research only DC resistance measurements are conducted.

To understand the resistance of where the asperities touch each other, it's important to have a look at the Holm A-spot in the semi-infinite circles model [7] (Figure 3.3a) and the A-spot in the thin film model [8] (Figure 3.3b). First, let's talk about the cylinder model, it consists of 2 main conducting current channels (region II and III). The cylinders are connected by a small bridge region (region I), if the limit of $h \rightarrow 0$ we approach the Holm a-spot [7], this spot represents the size of the current path between 2 bulk conductors. The same limit of h can be applied to a thin film (Figure 3.3b).

Why are these models are important for the contact resistance that's being investigated in this research? They mathematically describe what happens at the locations where the aforementioned asperities touch each other. In this way can the general idea of current paths created by touching asperities can be proven up by a mathematical relation. To achieve better conduction between two (dissimilar) materials more a-spots and/or bigger a-spots are desired.

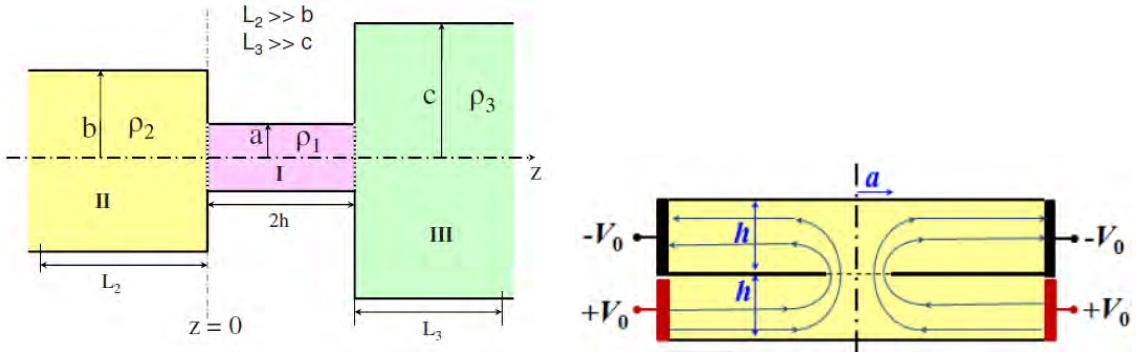

(a) Semi infinite cylinder model in the DC case [7]

(b) Thin film model in the DC case [8]

Figure 3.3: Two DC interface resistance models

Furthermore, each of the two transitions resistances[1] from Figure 3.3a can be calculated by solving Laplace's equation for the region: $z = -L_2$ to $z = L_1$. The schematic overview can be seen in Figure 3.4. The solution to this equation gives this expression for the total resistance [7]:

$$R = \underbrace{\frac{\rho_2 L_2}{\pi b^2}}_{\text{Bulk}} + \underbrace{\frac{\rho_2}{4a}\overline{R}_c\left(\frac{b}{a}, \frac{\rho_1}{\rho_2}\right)}_{\text{Interface}} + \underbrace{\frac{\rho_1 L_1}{\pi a^2}}_{\text{Bulk}} \tag{3.1}$$

The resistance relations for the regions: II, I, and interface of the schematic overview in Figure 3.4 can be seen in Eq. 3.1. If we express this interface resistance as $R_c = (\rho_2/4a)\overline{R_c}$ for the cylindrical channel, we find that $\overline{R_c}$ only depends on the aspect ratio b/a and the resistivity ratio ρ_1/ρ_2 [7]. Figures. 3.5a and 3.5b show that for a bigger a and for a smaller resistive-ratio

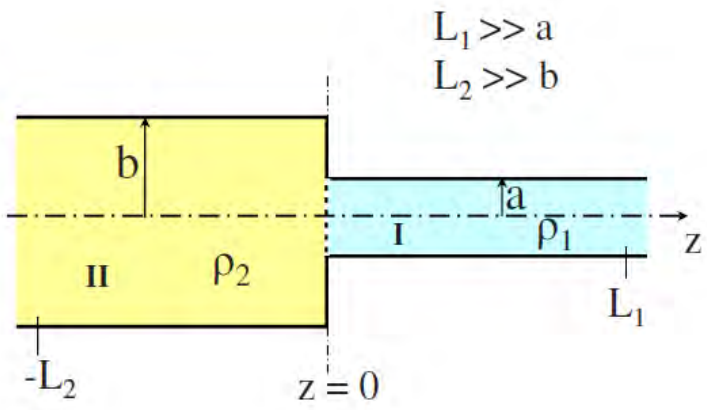

Figure 3.4: Semi-infinite current channel with dissimilar materials, regions I and II, in either Cartesian or cylindrical geometries. Current flows from left to right. [7]

that the normalised contact resistance will also be lower. Furthermore, from these two figures can be seen that the contact resistance depends more on the $\frac{b}{a}$ ratio instead of the ρ_1/ρ_2. In the case of this research is the ρ_1/ρ_2 limited to the available material combinations, but the $\frac{b}{a}$ could be made as low as possible by changing the physical size of the contacts.

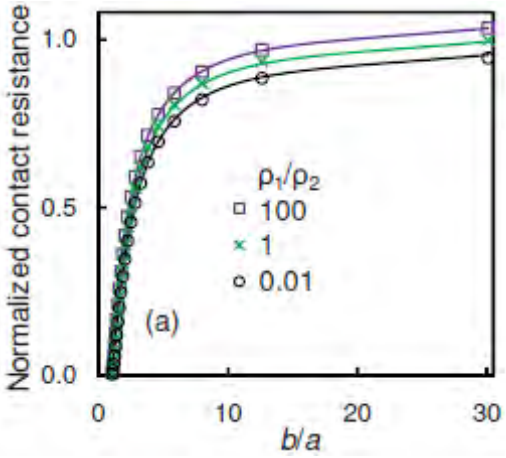

(a) The results of varying the area's: **a** and **b** compared the normalised contact resistance.

[7]

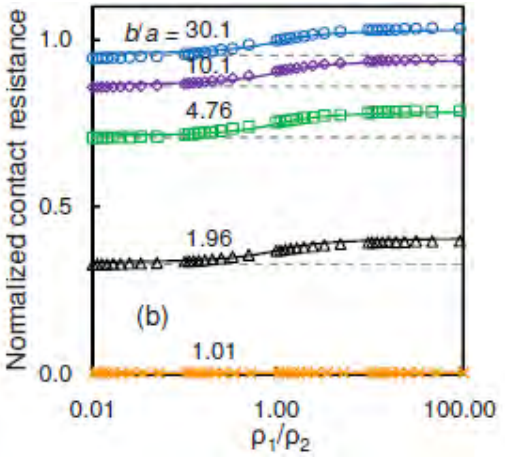

(b) The results of varying the restive ratio with: ρ_1 and ρ_2 compared the normalised contact resistance.

[7]

[1] region II→ region I or region I → region III

3.3 Mechanical interlocking

The literature covered above is mainly aimed towards the electrical properties, so i.e. which properties would make a good electrical connection. But to make the contact also mechanical reliable, some sort of adhesion needs to take place between the conductor and the conductive polymer. Figure 3.6 shows a schematic representation of what a reliable mechanical connection of two dissimilar materials could look like.

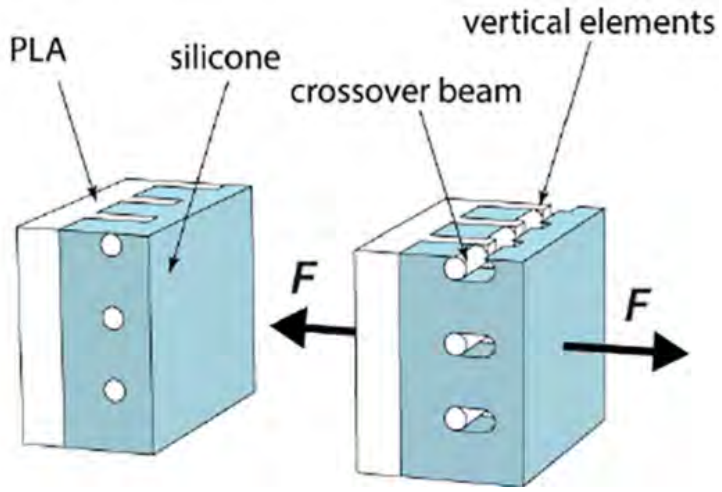

Figure 3.6: The mechanical interlocking (overmolding) of PLA and silicone in order to form a strong mechanical connection [9].

In the example from Figure 3.6 silicone is used as a flexible material, that is injected around a structure made of PLA. But for the application of this research, a similar structure can be used. But instead of extruding silicone out of a syringe, the 3D-printer could extrude hot conductive polymer into such a structure and form a mechanical reliable bond.

3.4 Theory clarification experiments performed by others

With now a base understanding of which parameters (geometrical and material properties) have an impact on the contact resistance between two dissimilar materials, its important to look at experiments performed by others. Experiments that can help to give a base understanding, taking into account the aforementioned electrical and mechanical theory.

The first experiment that is taken under the scope is an experiment where a piece of foam is coated in a PEDOT:PSS based conductive material [10]. The results of the experiments support the core idea that you can improve your conductance by pressing more asperities together. Since the coated foam is very porous [10] in the decompressed state a set amount of particles are conducting, but when the foam is tightly pressed together then more of the asperities can touch and so, more and/or larger conducting a-spots could be created. The results of compressing and decompressing the foam and recording its resistance change can be seen in Figure 3.7. The results of this experiment in Figure 3.7 would indicate the importance of having a tightly packed material full of conducting a-spots. The squishing would increase the amount of touching asperities and the results show that the resistance indeed decreases.

The foam used in experiments from Fig 3.7 doesn't fit the mechanical stable and robust contact application that is desired for this research. So a further look is needed, a look at another experiment where a bunch of concepts are tested. The methods and results can be seen in Figure 3.8. From these practical experiments can be seen that silver paste works the best in terms of electrical conductivity. However, it's not proven to be a mechanical reliable connection. Another important remark is that the copper tape and silver paste concepts were the only ones that did

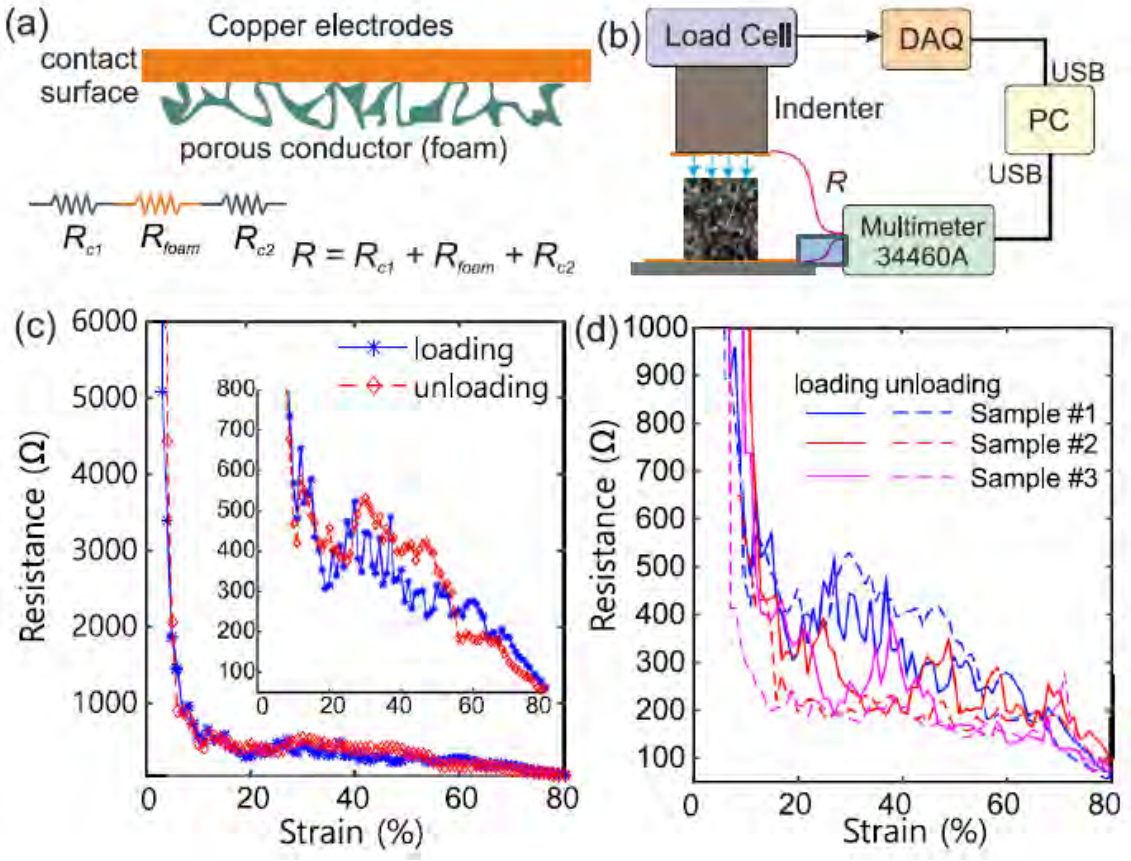

Figure 3.7: (**a**) shows the schematic resistance of the measurement setup. (**b**) show the equipment used in this measurement setup (**c**) and (**d**) show the results of compressing and decompressing the foam test sample [10]

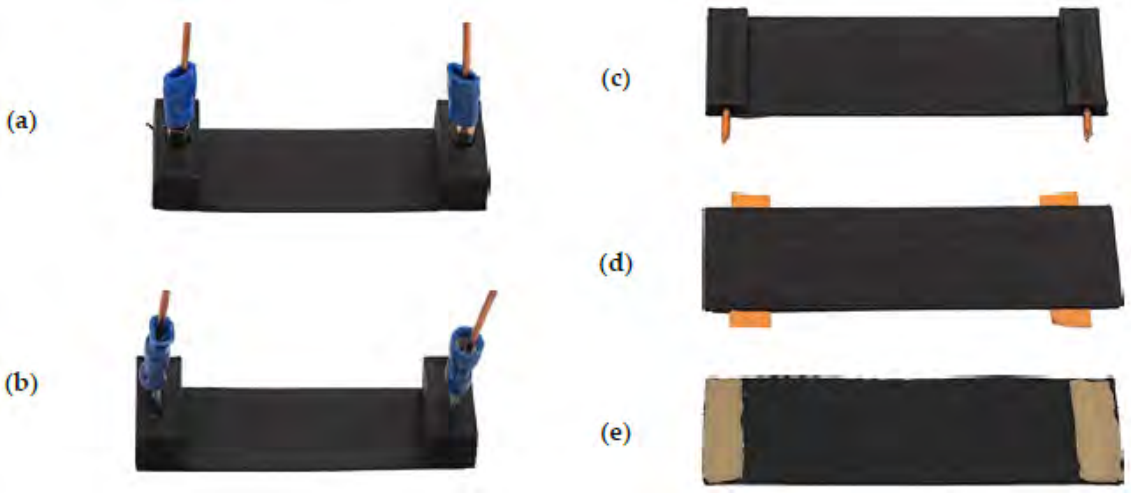

Figure 3.8: Illustration of the different investigates variants of electrical bonding (a) crimp connector (barrel), pressed in; (**b**) crimp connector (spade), pressed in; (**c**) copper wire pressed in; (**d**) copper tape, inlaid during printing; and (**e**) silver paste, applied after printing. [5]

not have a fluctuation in their values (based contact pressure). This would indicate that those two concepts are worth investigating further.

Table 3.1: Results of the experiments seen in Figure 3.8. Note: samples No. (**o**),(**a**),(**b**), and (**c**) are dependent on the amount of pressure by the probes applied during the measurement.

Sample No.	Name of Electrical Bonding Variant	Resistance
(o)	Without electrical bonding	6850-8500
(a)	Crimp connector (barrel); pressed in	403-597
(b)	Crimp connector (spade); pressed in	845-1209
(c)	copper wire (diameter 1.3 mm); pressed in	963-1504
(d)	Copper tape (width 5.5 mm); inlaid during manufacturing process	791
(e)	Silver paste (EMS 12640); deposited after manufacturing process	50.5

In the experiments with the foam samples and the experiment using different bonding methods, the total resistance is measured. It's important for these concepts that in this report the contact resistance is separated from the bulk conduction that takes place inside the conductive 3D-printed test piece. Furthermore, these experiments do not show the mechanical reliability of these concepts i.e. how many strain cycles would it take to break a wire off or something like that. For this report, it's therefore important to have both properties: electrical and mechanically stable and predictable.

To close of this chapter, the ram sensor investigation are presented below, these tables will be elaborated further in the next chapter (Phase I)

Table 3.2: Part 1/2 of the condensed version of the original RaM sensor investigation, which shows important electrical and mechanical properties of what sensor contact needs to be designed

Paper	Sensor(s)	Material(s) used	Resistance /Impedance	Connection Type	Size contact pad
Research into 3d printed batteries though electrodeposition	3D printed battery	ProtoPasta Conductive PLA	310ohm	silverglue and tape	1.5x1.5cm
Characterizing the Anisotropic Electrical Properties of 3D Printed conductive Sheets	FDM whisker sensor	ETPU and NinjaFlex	N/A	Print-In	8x8mm
	FDM, sEMG Electrode	ETPU and NinjaFlex	N/A	Mechanical	0.4x5mm
	Flash Light Circuit	ProtoPasta Conductive PLA?	N/A	Print-In	1x2mm
3D printed flow sensor	Robird flow sensor	PI_ETPU	1.8kohm	Copper tape with silver ink and solderedering	5x10mm
Magnetic field sensing on 3d printed structures	Hall effect Sensor	PI-ETPU 85-700	16-30kohm	Copper tape silverglue and solderd	5x8mm

Table 3.3: Part 2/2 of the condensed version of the original RaM sensor investigation, which shows important electrical and mechanical properties of what sensor contact needs to be designed

Paper	**Sensor(s)**	**Material(s) used**	**Resistance /Impedance**	**Connection Type**	**Size contact pad**
Development of PI ETPU based sensors for prosthesis control	prothese sensor; wristband		3400-2700 ohm (freq range 0-3000Hz) Max 6500 ohm Min 2000 ohm	Mechanical	10x10mm
3D printed implementation of a tactile pressure senor workin in muliple DOF	Whisker	PI-ETPU	0-10^5 ohm (freq range 0-1MHz) Max 70kohm Min 5.33kohm	Print-In	5x10mm
	FFS band (Strainguage)	PI-ETPU	4.2kohm	N/A	5x3mm
	tactile whisker	ETPU	MAX 160kohm MIN 20kohm	Print-In	5x5mm
3D printed Flexible Fingertip Strain Sensor	Strain sensor		MAX 3,8Mohm MIN 5kohm		3x5mm
Design, fabrication and characterisation of a force-sensitive sensor from inhomogeneous 3d printed matrial	Force and capacative	ETPU	1k-100kohm freq range 0-10MHz	Mechincal and Print-In	2.54x8mm
3D printed Shear force sensors	shear force sensor	PI-ETPU	10^6 - 10^4 ohm (freq range 1Hz-1Mhz)	Print-In	10x10mm
	shear force sensor		10^6 - 10^4 ohm (freq range 1Hz-1Mhz)	Print-In	5x5mm

4 Phase I - Exploratory research into, conductor and conductive-filament connections

4.1 Introduction

This chapter will cover the exploratory phase of the research, in this exploratory phase, based on the RaM sensor investigation summary (Table 3.2 and Table 3.3) a suitable contact area and conductor is chosen. On this suitable contact area are different contact joint concepts tested, including the silver paint that gave such promising results in the previous chapter. The printed traxels in this phase will be single width (one traxel of 800 µm wide) or double width. No large conductive body's like the experiments of Figure 3.8 will be used for this phase. This, was decided in order to study the mechanical adhesion between the surface (so no encapsulation) of the conductor and the conductive polymer. And to keep any resistance calculations regarding the traxels as simple and understandable as possible.

4.2 Method

4.2.1 Surface treatments and print parameters

The available printer for the experiments is a heavily modified Ultimaker 2, this printer uses the slicer Cura [11], this is therefore the slicer used for all the 3D-printing experiments in this research. For the conductive filaments, were PI-ETPU [12] and ProtoPasta conductive PLA [13] available. PI-ETPU is a conductive TPU (as mentioned earlier ETPU for short), which is a rubber-like material and used in flexible applications. ProtoPasta Conductive PLA, is like the name implies a Conductive PLA (as mentioned earlier EPLA for short), used for stiffer applications.

The ETPU an EPLA have vastly different viscosity, but ideally, the materials should work with the same metal conductor to keep the experiments as consistent as possible. The metal conductor of choice 6.35mm wide copper tape (3M, [14]), this material can be stuck down on a test piece and printed over by the conductive polymer that the 3D-printer extrudes out of its nozzle. This, without shifting around or fraying as a non-solid core wire does. The thickness of the copper tape combined with its sticky property makes this an ideal conductor to embed into a layer of a 3D printed part. The nozzle used in the experiments is a 800 µm stainless steel nozzle made by E3D, this is the wear-resistant nozzle available for the experiments.

For a reliable electrical connection, the conductive polymer (filament) needs to spread over the surface of the copper tape, i.e. forming as many (large) Holm a-spots as possible. To form as many a-spots as possible and simultaneously test the mechanical surface adhesion between the polymer and the copper tape. Will the tape's suraface be treated with different surface treatments, these treatments will be mentioned later in the text. To investigate the adhesion of conductive polymer on the treated surface of copper tape, only 1 or 2 traxels per sample are printed. This means that the copper tape for the experiments of Phase I is not enclosed in conductive filament and therefore only the surface adhesion between treated tape and the conductive polymer is investigated. The tape has been treated with the following techniques:

- Polishing the surface
  Note: *this method is not further investigated in this report because the polished sample did adhere very poorly to the conductive polymer en could be peeled off with not a lot of effort.*
- Rouging up the surface with different grid sandpapers (220 and 400 grid).
- Applying silver paint to the surface of the copper tape and printing over it.
- Using a self-designed SLA printed knurling wheel to make ridges in the tape.

- Punching holes in the tape to let the filament flow through the holes.
  Note: *The method of how the holes are punched is discussed later in the report.*
- These combinations of these above-mentioned elements: sanded copper tape 220 and 400 grid combined with the knurled wheel and silver paint; knurled wheel with silver paint; sanded copper tape 220 and 400 with knurled wheel

Not all combinations that are mentioned in the list above, will be worked out and discussed in this report. If there is no further elaboration on one or more of the above mentioned treatments they simply did not suffice to be investigated further.

To investigate as many scenarios as possible, Also a few print parameters are altered to see whether the mechanical adhesion between conductive polymer (filament) and the treated copper tape's surface could be optimized. By this is meant that when I was pulling on the traxels or even removing the print from the print-bed that the traxel already broke lose from the tape or lost significant electrical properties (drastic increase in resistance.), before proper processing was successful.

The following print parameters were altered:

- Nozzle temperature: 230°C, 240°C, and 260°C
- Bed temperature: Room temperature (22°C), 40°C, 50°C, 60°C, 70°C, 90°C, 100°C

All of the remaining print parameters e.g. extrusion-multiplier and layer-height were tweaked till they had an optimal value. These optimal parameters were then used for the rest of the test-prints in phase I. changing those print-parameters experimentally could have led to disruptions of the printing process e.g. clogged nozzles/scraping nozzles etc.

The layer-height for the experiments in Phase I was a fixed height of 200 µm, the reason for this was to give the second nozzle some headroom and preventing it from accidental scraping the copper tape which has a 66 µm thickness [14].

4.2.2 The print setups

Important note:*The images used in this section, can contain more than one surface treatment for example ridges with silver paint, sanded ridges, or sanded ridges with silver paint. Therefore the images have to be considered as only depicting an overview of how the samples were printed, without looking explicitly at the surface treatment. When the treatment is important it is specifically mentioned in the text or the figure's caption.*

Because of the undesired sensitivities of used the conductive filaments (dependency on temperature, moisture, etc) used in these experiments, it's important that the conditions i.e. the combination of the print temperatures, and the tape's surface treatment are tested quantitatively. This, to see whether a trend or pattern exists in multiple print runs. Furthermore, all possible parameters (including environment variables) are documented. Figure 4.1 shows one of those the tables that were used to document all critical parameters, pre- and post-printing.

For the first batch of experiments a simple non-conductive frame (made of PLA) with indicators is printed with the printers secondary nozzle, this can be seen in Figure 4.2 (red circle). With this frame in place the treated copper tape can be placed during a pause of the printer in the appropriate location, so guided by the frame. This frame also contains small tabs (Figure 4.2 green circle) that indicate how far the two strips of tape need to be spread apart, to improve the consistency of the tape's placement. The distance between the two lines of tape is chosen to be one 400 µm secondary nozzle line width.

RUN	A			Date			9-6-2020			
Printer Settings				Environment						
Track Height	200		µm	Room Temp			22.6			°C
Retraction Length	0		mm	Relative Humid			41.9			%
Retraction Speed	0		mm/s	Glass Plate Temp			28.2			°C
Print Speed	5		mm/s	Silver Paint			~~YES~~	NO		
Exturder Multiplier	150		%	Probe Offset			0.2			Ω
Bed Temp	40		°C	ρ-Material			375			Ωcm
Print Temp	240		°C	Calculated Resistance			2407.33			Ω
Material	ETPU			Cleaning Copper			IPA			
Track ID	1	2	3	4	5	6	7	8	9	10
Track Width [µm]	1860	1840	1910	2100	2000	2000	1820	1840	1760	1960
Track Height [µm]	200	200	200	200	200	220	210	210	200	200
Tape Gap [µm]	250	250	250	250	250	250	250	250	250	250
Mearsured R per track[Ω]	4100	3600	1900	1800	2000	1400	2100	2300	2700	2000
Calculated R per track [Ω]	2520	2548	2454	2232	2344	2131	2453	2426	2663	2392
Average Measured	2389.8		Ω	Difference				17.5275		Ω
Remarks	After pulling up on track 5 medium force the maximum resistance reached 4100 ohm after relasing the pull the resistance fluctuated between 2000 and 4100 ohm Pulling the copper tape off wasn't to hard compared to sampe C									

Figure 4.1: This image shows how a batch of test prints is characterized. Furthermore, in the remark section is noted down how good the traxel did stick down to the surface of the copper tape.
NOTE: *In this table only 10 tracks are noted down were later in this section 20 traxels per batch are printed. The experimental set-up changed from 20 to 10 traxels, since 20 traxels required too much preparation for each batch. Hence, why this table only shows 10 traxels*

This very narrow gap reduces the influence of the conductive traxel that bridges the gap between the two pieces of copper tape. This bridged conductive polymer is not touching any of the copper tape's surfaces and therefore not helping to improve the contact resistance between polymer and tape. Therefore this gap is desired to be as small as possible. For each run 20 tracks were printed (later reduced to 10) on the treated copper tape mentioned in section 4.2. Then those batches are categorized in the therefore designed data collection tables, like in Figure 4.1.

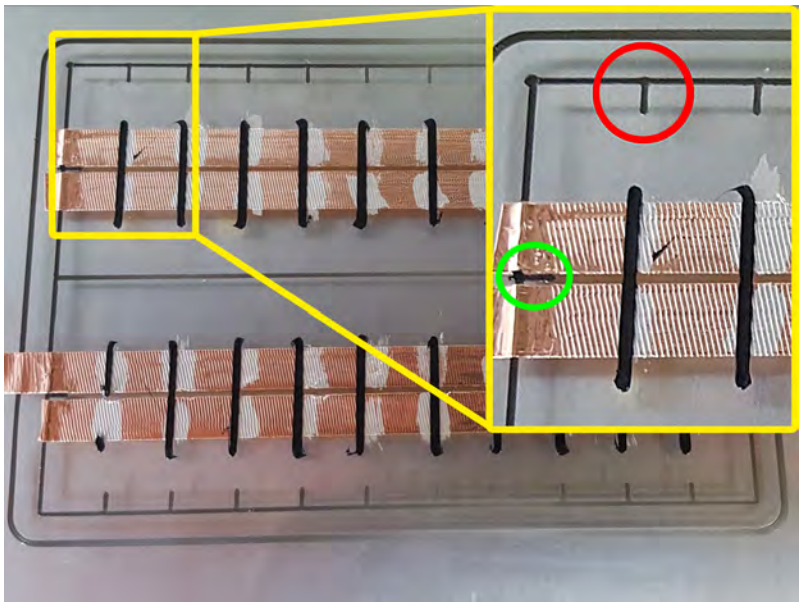

Figure 4.2: A non conductive frame with registration lines (red circle) that indicate where the conductive traxels will be printed.

The resistance of the tiny bit of material that bridges the gap between two strips of copper tape (green circle in Figure 4.3) can be calculated with its dimensions and volumetric resistance (ρ). A multimeter (BRYMEN BM869s) is used to measure each traxel individually to see if the previously mentioned calculation lies in the same order of magnitude as the measurement. The measurement is done by connecting the gold plated multimeters-probes to the isolated copper tape islands, which are shown later. Any deviation could be the cause of the poor contact, this is exactly what this research is trying to investigate. To measure each traxel individually, the tape has to be sliced so each traxel is isolated from its neighbour, this can also be seen in Figure 4.3. It's important to mention that only DC measurements are taken from the tracks.

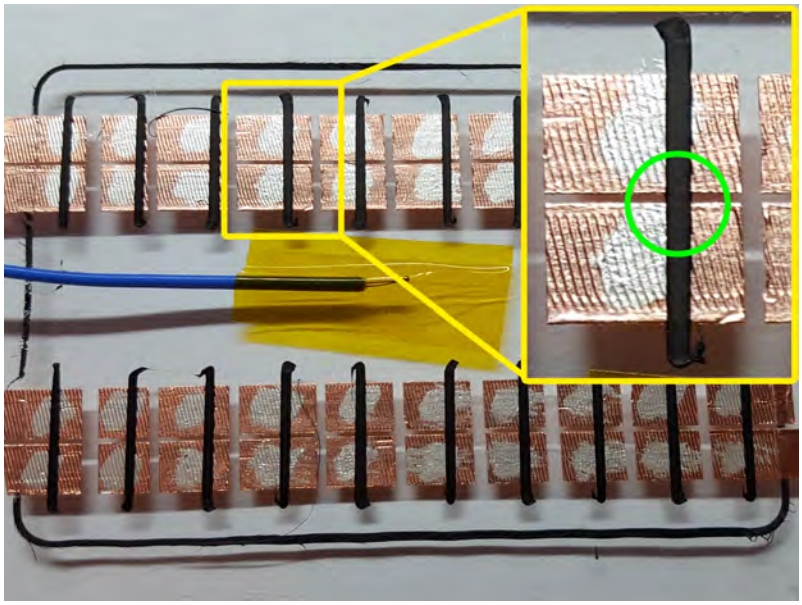

Figure 4.3: The 20 tracks were cut loose to be able to take a DC resistance measurement on each of them, a thermocouple is added to measure the temperature of the glass plate for documentation.

For the treatment where holes were punched through the copper tape, a different print setup, from which the latest CAD model can be seen in Figure 4.4. Figure 4.5 shows the print before the nozzle with ETPU or EPLA prints over the holes (note: this is a slightly older version of the design in Figure 4.4).

Figure 4.4: latest iteration of CAD model used to do the 10 sample test prints, model is both for ETPU and EPLA suitable. The black stripes are the printed conductive polymer traxels, that are printed on a white non-conductive base layer

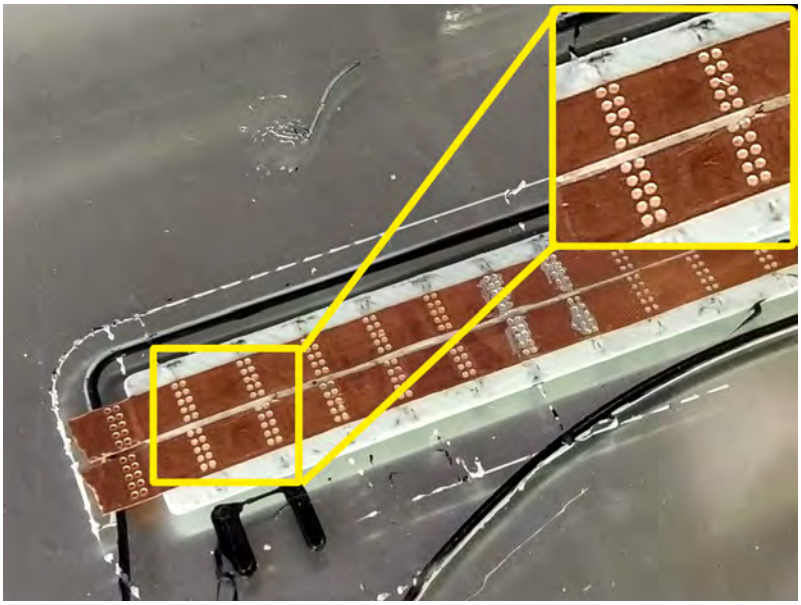

Figure 4.5: A picture before printing with the conductive filament, each track has 10 holes of 600 µm per strip of copper tape where the conductive filament can flow through the holes. And adhere to its base layer made of PLA or TPU respectivly.

For punching the holes in the tape an SLA printed jig was used, this jig can be seen in Figure 4.7. For the punch itself (the needle) a 600 µm hardened sewing pin is used, from which the sharp point is cut off with a pair of snippers and the snipped of the end is sanded flat. This ensures together with the jig that a clean hole is punched in the tape. By this is meant that no burr will be created after punching that could be pushed back over the hole when sticking down the tape, that could partially block the hole. A schematic overview of the punching can be seen in Figure 4.6

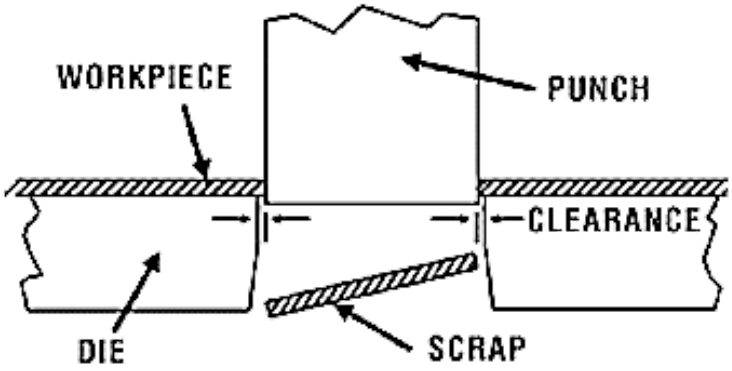

Figure 4.6: This is a schematic overview what happens inside of the punch [15]

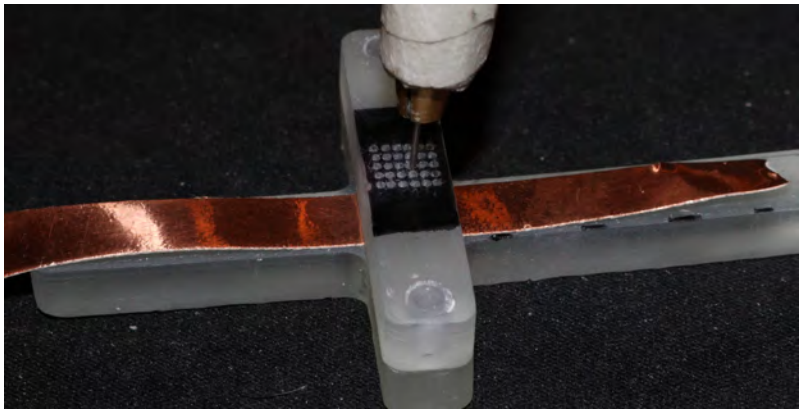

Figure 4.7: The custom made hole punch with small tabs (highlighted with black sharpie) that indicate the spacing for each hole pattern, the actual tabs are to small to see without zooming in, the CAD model of this jig was put in Appendix A in phase I extra's

To achieve the best adhesion for this setup a base material that is made out of same polymer as the conductive polymer is desired i.e. for the ETPU a base layer of TPU (NinjaFlex) and for the ProtoPasta a base layer PLA. For practical applications could the conductive polymer be used for both e.g. the base layer is made of the same conductive polymer as the layer covering the holes. With the perforated copper tape setup, the conductive filament can be pushed through the holes by the nozzle the result after printing with the conductive polymer can be seen in Figure 4.8.

The traxels used in the experiments which do not involve holes are 1 traxel wide (800 µm) compared to 2 traxels that are used in the experiments that involve the perforated tape. These double traxels are there to make sure that a sufficient amount of material would flow through the holes. Even with a slight misalignment of the hole pattern in comparison to the path of the nozzle.

Figure 4.8: 10 ETPU tracks (black) printed over the punched holes in the copper tape connecting to a NinjaFlex base layer (white)

4.3 Results

All of the aforementioned copper tape treatments except for the perforated hole design failed just by simply pulling on the traxels with a pair of tweezers. This became clear from the remarks in the data collection tables mentioned earlier. Most of the traxels that were noted down in these tables behaved as expected, i.e. resistance measurements and calculations did agree in the same order of magnitude. But just after messing with the sample (bending it back and forth), The results are simply not reliable, even the slightest of movement will tear the traxel lose and therefore drastically increase the contact resistance and therefore make the resistance value of the test not relevant. Figure 4.9 shows why initially was believed that some non-perforated tape's surface treatments had worked.

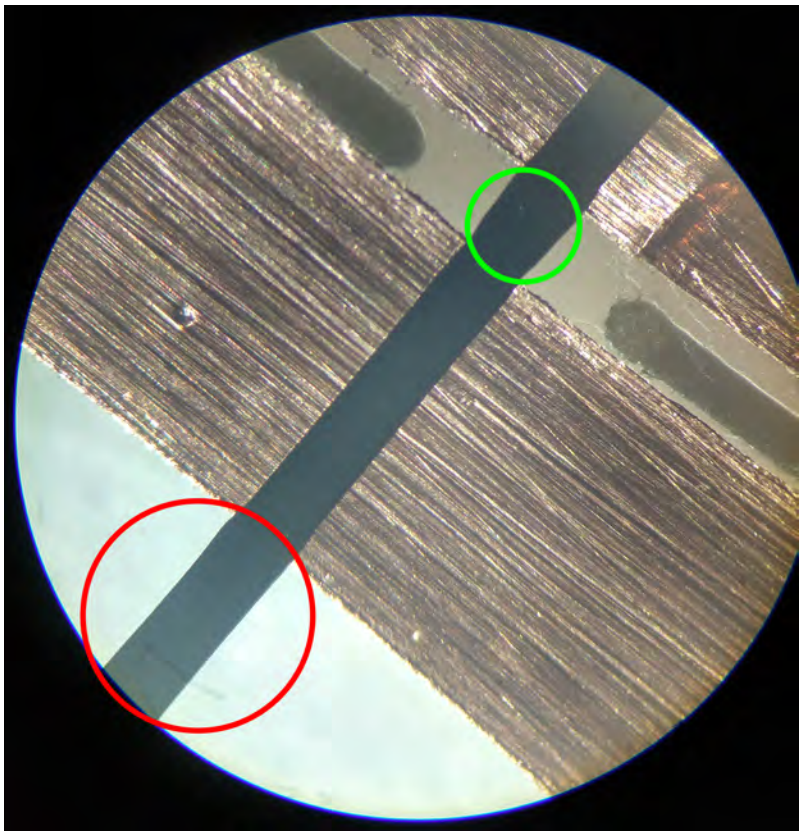

Figure 4.9: Sanded copper tape with 220 grid where the red circle shows the end of the tracksel and the green circle shows the location where the track bridges the gap from one tape strip to another.

The locations where the traxel touches the treated build-plate (with 3D Lacker), depicted in the red and green circle. Did make it look like that the traxel properly adhered to the copper tape. While in reality, the places were the filament was overshooting the tape the actual bonding did happen. By carefully pulling on the traxel with tweezers starting in the red circle, the traxel gave way at some point and then stopped at the location in the green circle. This is suggesting that the traxel adhered to the treated glass instead of the treated tape. By investigating the track under a microscope (Figure 4.10) the impression of the sanded surface could be seen in the filament.

NOTE: *The microscope used is binocular because the images only could be taken from one eye-piece the depth perspective is lost. With this it's much harder to convey the microstructures embossed by the surface of the tape into the filament.*

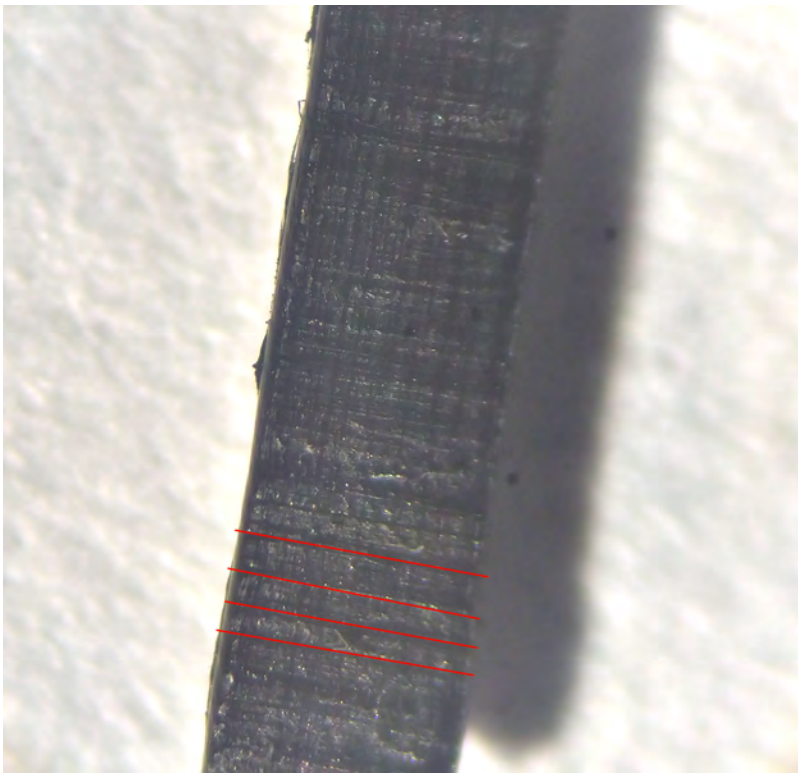

Figure 4.10: Microscope investigation of a single traxel pulled off a 400 grid sanded surface. The red lines subtly indicate the microstructes embossed in the surface by the tape

The result of the knurling wheel treatment, mentioned earlier gave the same result. However, the combination with silver paint did stick to the filament but not to the tape, this can be seen in Figure 4.11, so even with much courser ridges in comparison to sanding still the desired mechanical adhesion between conductive polymer and copper tape was not achieved. Even by changing the temperatures from the bed and the nozzle to many sane and even insane temperatures, starting at the bed at 22°C and raising it to 100°C.

After pulling on the separated contacts (Figure 4.8), used in the experiments that involve the perforated copper tape, a noticeable change in resistance could be seen. For the much stiffer ProtoPasta (EPLA) this change was instant and permanent after applying force. For the softer ETPU only after stretching too so much that the change in resistance became permanent. Because this process of pulling and flexing the samples is not scientific enough no concrete results tables are added to this report. However a few ETPU sample data collection tables are added in Appendix A in phase I extra's, to give an idea of what kind of information the tables would give. The test in this phase were mostly used as a guide to finding the right direction to move in.

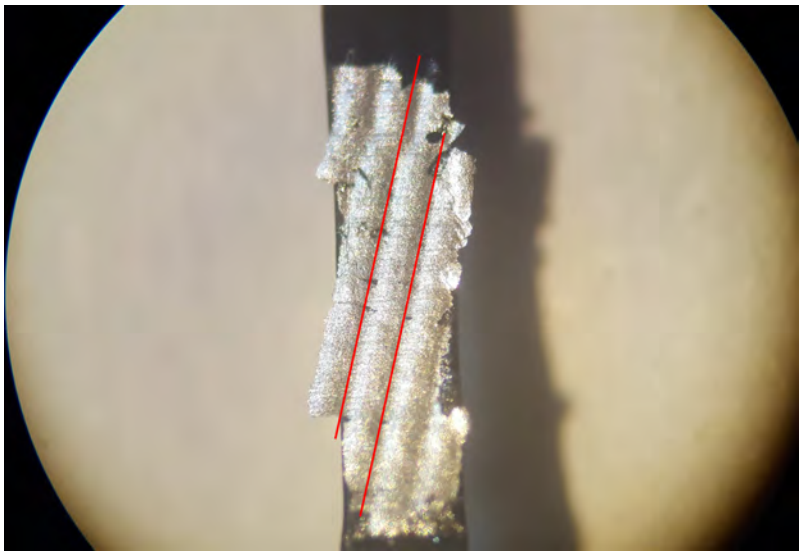

Figure 4.11: You can clearly see the diagonal knurling pattern (red lines) but all of the silver tape is stuck to the conductive traxel. On the tapes surface there was a strip of paint missing (unfortunately no picture was taken form this).

By pulling the perforated tape sample off the white base layer, black dots could be seen as a remainder. This could indicate that the extruded conductive polymer was properly fused to the base material, the dots can be seen in Figure 4.12. Where the non-perforated samples failed at the contact interface, did the interlocking (perforated tape) samples fail at a material level, e.g. the conductive polymer did break lose from itself.

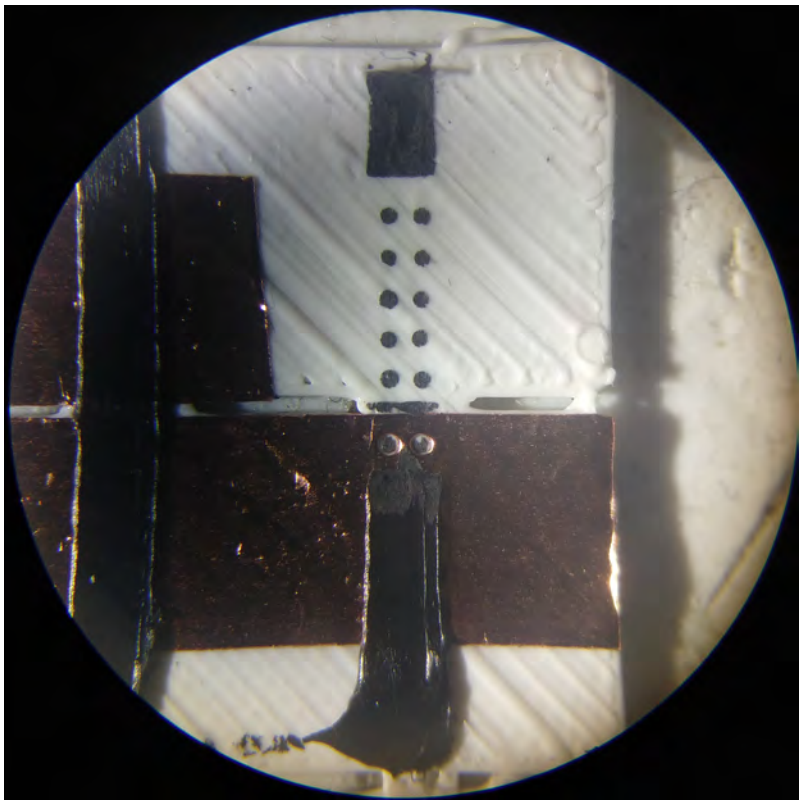

Figure 4.12: The 10 black dots indicate that the fusion of EPLA on the PLA base layer(white) was successful

In order to have a look at what would happen at a materials depth perspective i.e. how deep the EPLA would penetrate the the base layer in white. A razor is used to cut the sample open, a cross section of such a EPLA perforated test sample can be seen in Figure 4.13

Figure 4.13: A EPLA test sample cut off with a razor blade in order to have a look at the cross section of the polymer extruded through the holes. The green circles indicate where this has occurred.

The sufficient fusion of conductive polymer and non-conductive polymer did not happen 100% of the time it's important to note that this fusion became strong over 65°C of bed temperature, for the ProtoPasta filament. For this fusion it's important that the tape and base-layer is heated up to at least this temperature. A lower bed and therefore environmental temperature would let the extruded conductive polymer cool down to fast and not properly fuse to the base layer. This means after pulling the copper tape with the traxels you could not see all 10 dots on the base layer, this can be seen for the ETPU samples in Figure 4.14. Stating that the bed temperature is slightly lower for ETPU than the mentioned 65°C for EPLA, this will be explained further in this section.

Figure 4.14: [**NOTE:** bed temperature 40°C] Here you can see that in the green circle the fusion was properly, you can clearly see more black dots than in the red circle, 1 row of dots is entirely missing.

As mentioned earlier proper fusion only happened with a sufficient temperature from the build-plate. The test print that was printed in Figure 4.14 was printed with a bed temperature of 40°C, for a higher bed temperature it was harder to pull off the tracks from the base layer. For the ETPU samples, a bed temperature of 60°C made the bond so strong that the tape just tore, this can be seen in Figure 4.15.

The nozzle temperature was set to a 230°C for the ProtoPasta filament (EPLA) and the PI-ETPU filament to 240°C and 260°C, this high temperature did degrade the material, resulting in a brittle traxel (table D, remarks in Appendix A in phase one extra's).

Figure 4.15: [**NOTE:** bed temperature 60°C] In the red circle you can see that the fusion between the ETPU and the Base layer (TPU) is so good that the tape just simply is pulled away from the connections so the 10 stakes stay in place and the tracksels are still attached.

4.4 Discussion and conclusion

With many different methods tested it was not possible given the time and the integrity of the samples to do a proper quantitatively test and use the tables that were shown in Figure 4.1. The results of the samples were foremost good, hence some of the ETPU characterization tables were put in the Appendix. However, due to the fragile nature of the non-perforated copper tape samples, would even the slightest stress on the samples degrade the connection between the conductive polymer and the tape drastically. Only the method with the perforated copper tape does have enough mechanical interlocking strength to maintain a large portion of its electrical properties after bending and pulling on the samples, this could also be seen in the data collection tables in the remarks (A,B,C, and D) in the appendix A in phase I extra's.

Furthermore, only DC measurements were done in these experiments, impedance (AC) characterization would certainly add a lot of value to this research. However, due to the available time and the amount of work these AC experiments were not conducted.

At last, the perforated tape samples were printed on a 600 µm thick base layer (white in the pictures). Future sensors could require the copper tape to be embedded further from the heated bed and then the bed temperature of 60°C and 65°C respectively could not be sufficient enough for a proper fusion, this is something to keep in mind. The next phase will proceed with this concept of perforated copper tape.

5 Phase II - Dissimilar material connections by mechanical interlocking

5.1 Introduction

The previous chapter concluded that printing over a perforated strip of copper tape is a promising concept i.e. mechanical interlocking helps to construct a good mechanical stable contact. This chapter will investigate how this concept contributes to the mechanical integrity of the contact and which electrical behaviour can be expected. Furthermore, how many holes are needed to achieve a reliable electrical and mechanical connection. The samples in this chapter will be subjected to cycle testing i.e. loading and unloading the samples with a 1 kg wight to see how different amounts of holes behave over a long period of cycle testing.

5.2 Method

5.2.1 Choosing a suitable test sample design to print

In this phase, it's really important to isolate the contact resistance from the rest of the test sample. This isolation is important because e.g. an ETPU (flexible) sensor can vary a lot in value and it's not desired that the contact resistance of such a sensor would contribute to this fluctuation. To understand what kind of resistances we are dealing with i.e. the total resistance of a test sample can be split up into multiple resistances in series, including twice the contact resistance. A schematic overview of which resistances are present in the measurement loop can be seen in Figure 5.1.

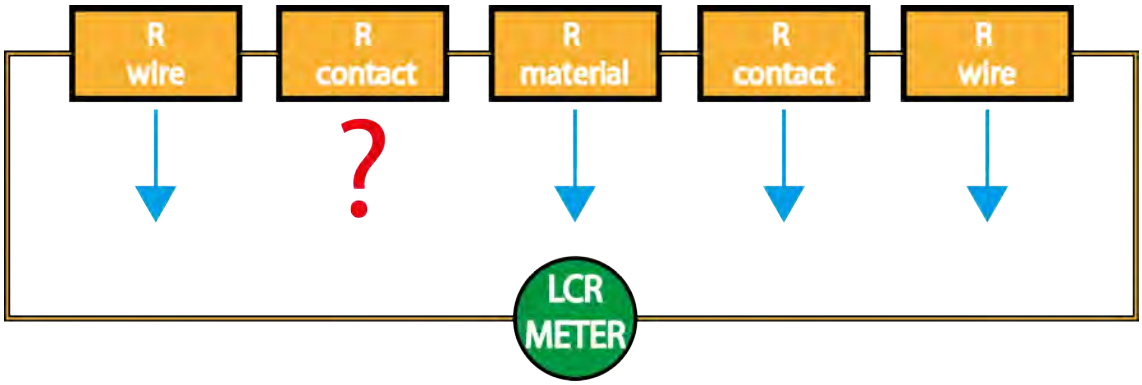

Figure 5.1: The resistances present in the measurement loop, the blue arrows indicate which resistances are low by definition or are going to be tweaked in such a way that they can be made low an most important trying to be made stable. The question mark represents the contact that is going to be investigated

The chain of resistors shown in Figure 5.1 starts and ends with a measurement wire coming from a LCR meter. This meter is used because it has a logging feature over USB and samples approximately 2 times per second. The meter is put in DC mode and the brand and model are: UNI-T UT612. The resistances of these wires is approximately 0.2Ω. This value is so low and foremost stable, so it can be neglected for these experiments. Both of the contact resistances are a completely unknown parameter in this loop. To measure one of the two contact resistances, one contact is constructed in such a way that the surface area of the tape is much larger than the other and that the tape is full of holes. This to reduce the contact resistance fluctuations, that can occur when the sample is put under load (during the cycle testing). An overview of the electrodes can be seen in Figure 5.2, where we have to take in mind that the tape has a width of 6.35 mm

Figure 5.2: This is what the test piece looks like before it's being covered by 1.25 mm of ETPU layers. Fully capturing the electrodes with holes inside. The amount of holes is varied in conductor 1 so what you see in the picture is not used for all tests.

The body of the test sample is desired to be as conductive and consistent as possible, this means that the body consisting of conductive polymer needs to be relatively big compared the contact that is being investigated. (indicated by the red question mark Figure 5.1). The dimensions of the test sample will be presented in the sample fabrication section. The size of conductor 1 is based on the RaM sensor investigation mentioned in phase I, this means making the contact relatively large to have sufficient surface area but be compact enough to be implemented into a robot sensor.

5.2.2 Sample Fabrication

The dimensions of the test print used are 40 mm by 30 mm by 2.5 mm. For the fabrication of the copper tape electrodes, yet another jig had to be designed and SLA printed. This jig makes it possible to puncture the large number of holes that are needed for conductor 2, but also able to be used to systematically puncture precise holes in conductor 1. This all-round punch jig can be seen in Figure 5.3.

Figure 5.3: Special designed jig to punch 600 µm in a controlled way in the copper tape. the jig ensures a constant alignment of the tape and allows the user to punch 10 or 1 hole at the time. The 10 hole punch is not included in the photos.

The CAD model of the jig, which also shows the hand piece of the punch can be seen in the Appendix A in phase II extra's. The jig, just like the first jig used in phase I, prevented the creation of a bur in the tape after punching as well. A clean round path will fall trough the bottom hole of the jig and can be removed when the jig is lifted. More photos of the jig can be found in Appendix A in phase II extra's

After punching the holes, is the copper tape stuck down onto a half printed test sample (printer is waiting with a pause command) before being fully encapsulated (with the other half of the print). The tape didn't stick very well on the hot ETPU test sample, which was still heated by the 65°C bed below it (during the printers pause). The holes make it possible to use a soldering iron @400°C) to gently touch a few holes to push a little bit of material through the hole. This fixes the copper tape in place mechanically, this can be seen as the black smudges on conductor 2 and 1 in Figure 5.2. These small "heat stakes" is what holds the tape down, the glue doesn't do to much. Note that these actions are conducted during the pre-programmed pause of the the printer half way in the print cycle. After the print is resumed and the printer finishes the test-sample, they look like Figure 5.4

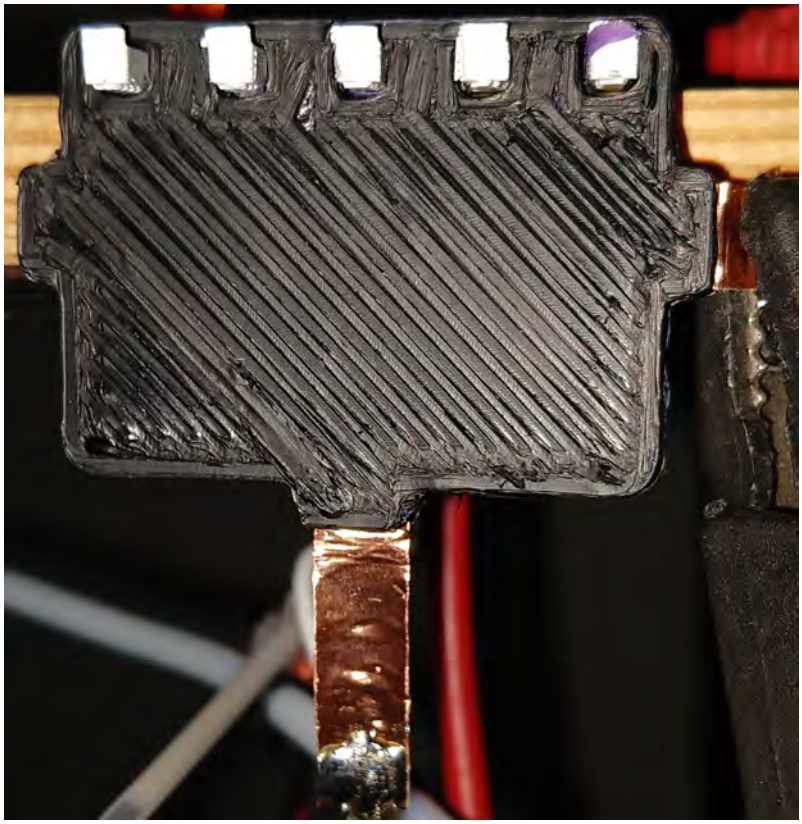

Figure 5.4: How a finished phase II test sample looks like.

5.2.3 Experimental set-up

The experimental set-up consists of subjecting the printed samples mentioned in the fabrication section to a multiple hours during, loading and unloading (so pulling and relaxing on the samples from the fabrication section) with 1 kg of weight, the duration of the loading and unloading is each 10 seconds.

For testing the samples mentioned in the previous section, a copper ring is soldered to conductor 1. This ring is there to attach the test weight of approximately 1 kg to the test piece (inside the yellow border in Figure 5.5). This bottle of water is then lifted by the 3d printer's bed, an overview of this setup can be seen in Figure 5.5. A piece of custom G-code based on marlin firmware to keep the build-plate up for 10 seconds and then down for 10 seconds was written. This test file could do the up and down movement repetitively for more than 10 hours. The test-samples were all printed in ETPU with the following settings:

Table 5.1: Printer settings used for the cycle testing samples

Bed Temperature	65°C
Nozzle Temperature	235°C
Extrusion Multiplier	110%
Print Speed	15mm/s
Layer Height	250 µm
Infill Direction	Alternating 45°

This multiplier setting did not turn out to be a great choice, the total resistance measured was much higher than anticipated. So further investigation is needed to find out where this unexpected high resistance comes from, this will be further elaborated in Phase III. The reason why ETPU is chosen as the test sample material of choice and not EPLA is: one, now widely used at RaM for wearables and flexible sensors. Two, the material stretches more than EPLA and could, therefore, be more susceptible to heavy deformations that could influence the contact resistance.

For all of the samples printed, the amount of holes in conductor 1 is altered, while the dimensions of the copper tape printed in place remained the same. The number of holes was incrementally increased the following way: 0,1,5,10,25 holes respectively. In addition to the tests with the holes, a wire was molten in with a soldering iron (set to 400°C) and then printed over by 1.25mm of material (as a control reference). The cyclic loading and unloading of the test samples was continued either: till something broke e.g. some samples had the copper tape ripped out of the sample. Or, over time, nothing significantly would happen anymore.

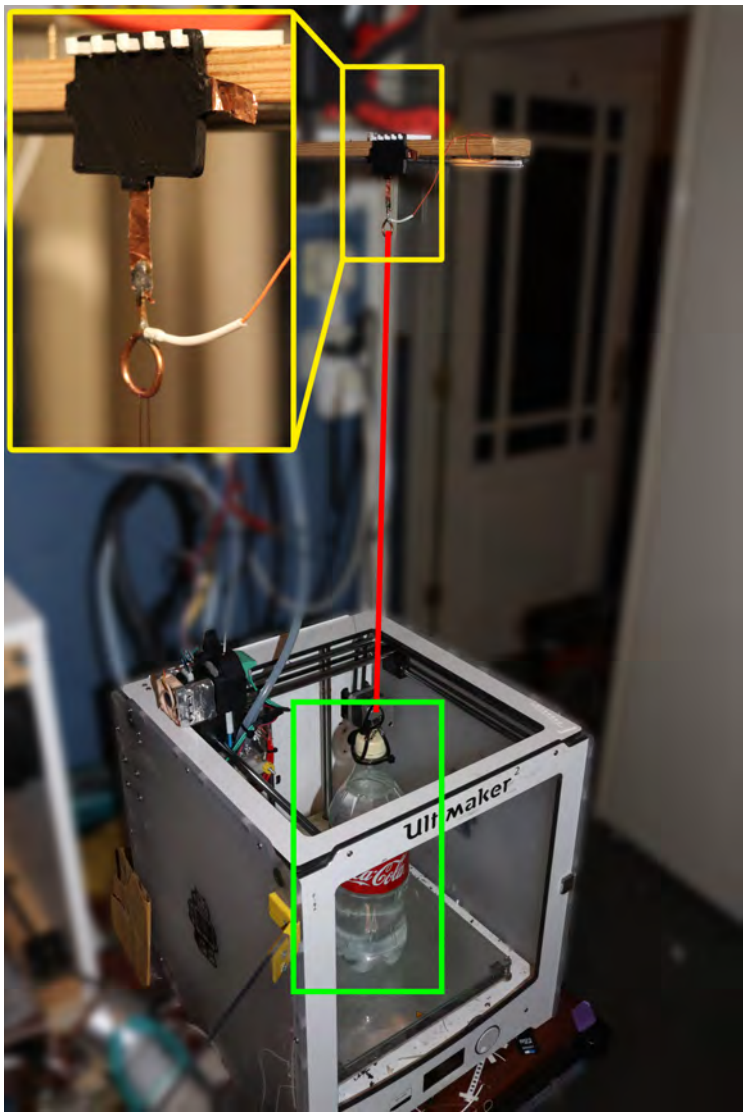

Figure 5.5: The test set-up for cyclic loading/unloading, with the test sample hanged from a beam and, where a water bottle is suspended from a fishing line and lifted and lowered by the printing bed.

5.3 Results

The results of the cyclic loading and unloading are put into 1 graph, which can be seen in Figure 5.6. In the graph can be seen that 4 out of the 7 test failed, the large spikes that shoot up imply that the contact is being ripped apart, i.e. the tape is pulled out of the test sample. An interesting thing to note is that the resistance value does increase before the contact will fail. Another interesting thing is, that the two-hole piece of tape did not last as long as one hole. The graph also shows that: the more holes punched in the tape, the lower the starting resistance is. and even more interesting even after making more than 1000 cycles the resistance remained lower.

Figure 5.7 shows a zoomed-in version of the graph in Figure 5.6, where the change in resistance can be seen as a result of loading and unloading the sample. This loading and unloading can be seen in the graph, the maximum change in resistance due to loading and unloading looks a bit higher for the samples with fewer holes.

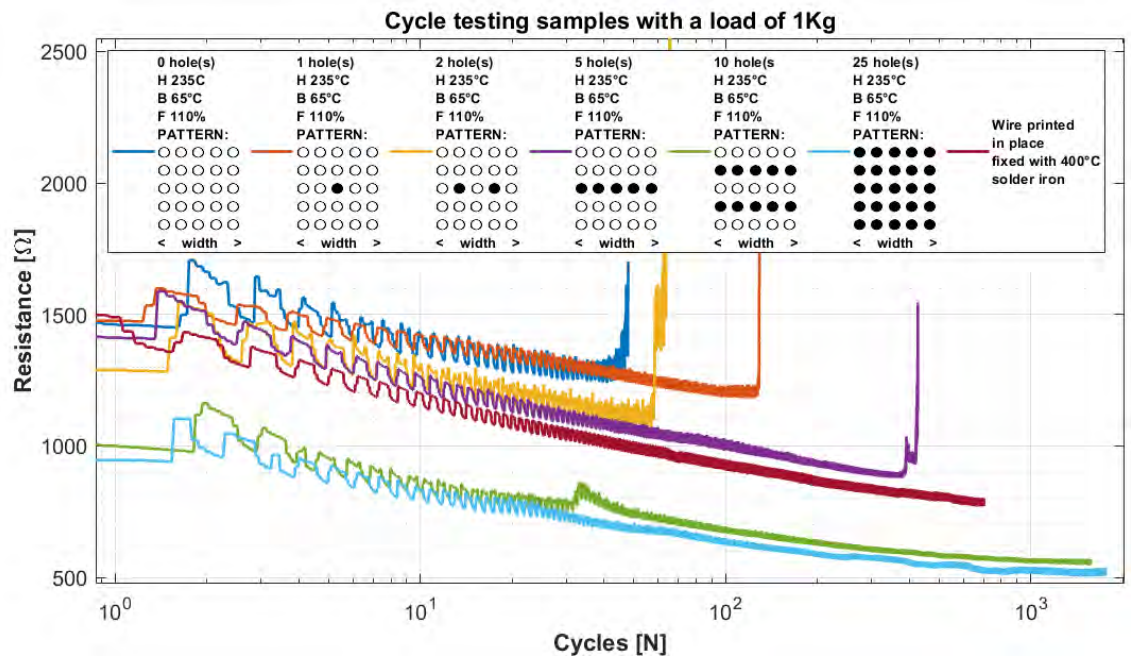

Figure 5.6: This image shows the results of loading and unloading the samples with 1 kg for 10 seconds. The pattern in the legend shows the hole pattern used, the word "<width>" means that this is the width of the copper tape, the black dots represent a location where ETPU filament is extruded through a hole. The clear dots are possible hole locations.

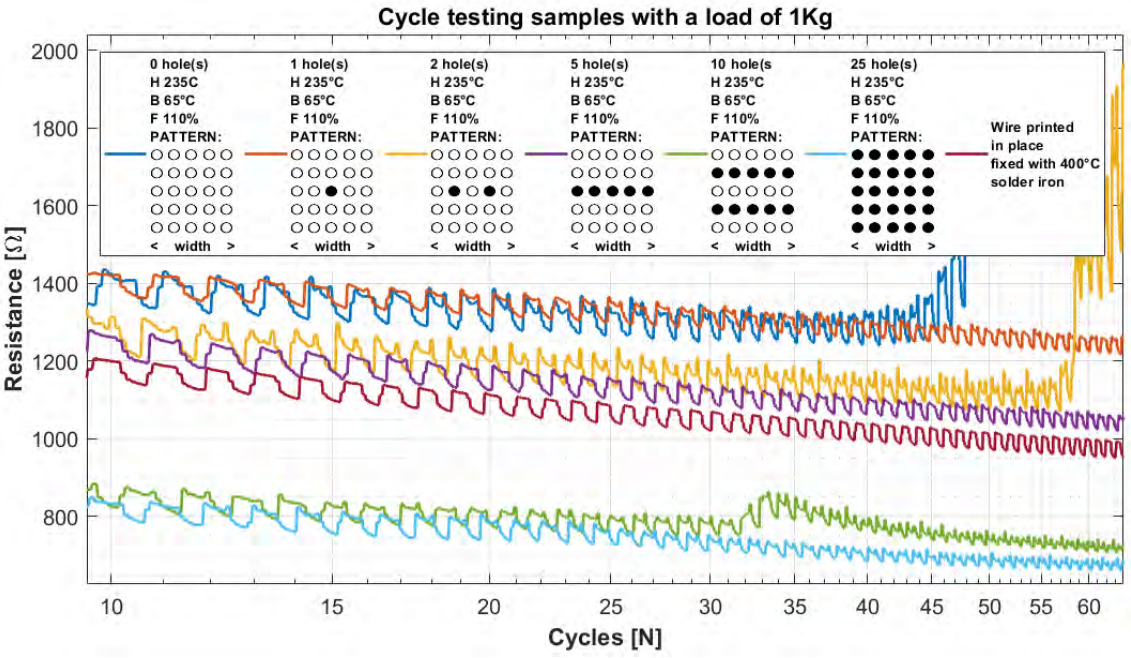

Figure 5.7: This is a zoomed version of Figure 5.6, this shows the change in resistance (periodic behaviour in the graph) per sample by loading and unloading the samples, with the 1 kg bottle.

5.4 Discussion and conclusion

The results of the cyclic testing were excepted for most of the samples, only the sample with 2 holes was unexpected. Nevertheless, From the results could be seen that more holes in the tape would achieve better mechanical interlocking paired with a more stable electrical resistance during the cyclic testing.

A very important note is: why do the resistance curves of the samples decrease in value over the number of cycles? This could be the cause of the samples still cooling down, however, even when the samples reached room temperature they still decreased in resistance over time. This "settling" behaviour of the samples is worth investigating in greater depth, this will, therefore, be done in Phase III (next chapter). In the method section, we spoke about making the resistances marked with a blue arrow as low as possible or at least consistent. From Figure 5.7, this however was not the case. The value of the samples almost all started in the kilo-ohm range. While the maximum deviation in resistance from loading and unloading the test samples was not more than $50-100\Omega$ of change between the minimum and maximum value (Figure 5.7).

This high starting value could be the cause of the extrusion multiplier, this value was set to 110% (to prevent under extrusion), while more conventionally this value would be set to 100%. Therefore will this setting be further tested in Phase III, to see if the extrusion multiplier affects the starting resistance of the samples and also on the resistance settling time which could be seen in Figure 5.6. To better track the printing process, a new method is introduced: the In-Situ resistance measuring (resistance measurement during printing).

6 Phase III - In-Situ Resistance Monitoring

6.1 Introduction

The previous chapter was closed with the introduction of a new method, the In-Situ resistance measurement of conductive test samples. This new method that could reveal were the unexpected high starting resistances of the samples could come from. By monitoring the print from the very moment that the electrodes make contact with the conductive polymer, it could be seen how the resistance develops itself during the print process, things like a hot nozzle moving over the print could cause temporary disruptions in the total resistance of the sample. In this way also the contribution of each layer can be seen to the total resistance of the print/sensor. Furthermore, the printhole could be monitored after the printing to see how long it take for a test sample to reach a consistent resistance value, i.e. extending the In-Situ monitoring to a post-monitoring situation.

The methodology for this chapter will consist of a section which started with doing In-Situ measurements on the samples from phase II, as a way of investigating where the unexpected high staring resistance would come from. Later, custom samples were designed that would be further tested and ended up in their research paper [16](Appendix A in phase III extra's).

6.2 Method

6.2.1 In-Situ measurements for the samples used in this report

So as mentioned in Phase II, that the choice of an extrusion multiplier of 110% did give the expected low starting value for the test sample. So for phase III, this extrusion multiplier is studied, the studied values used are 100%, 110%, and even 120%. To test this method, even more, the nozzle temperature is also changed a few times, to temperatures of 225°C,230°C, and 235°C respectively. To see if the temperature would also have significant effects on the starting resistance of the samples and investigate how the resistance changes from the moment the first layer is put over the test electrodes (named conductor 1 and 2 in Phase II).

The samples from phase II were all printed in PI-ETPU, however, to conclude the In-Situ monitoring more complete, two samples of ProtoPasta (EPLA) were printed and monitored as well. The setup used 25 holes in the smaller electrode during the measurements, So i.e. all samples that were monitored In-Situ in this section had the hole pattern that was shown in chapter 5 in Figure 5.2. The infill direction and print speed stayed the same as well compared to the samples in phase II (Table 5.1), namely 45°infill direction (so 45, 135°, 45°and so on).

6.2.2 In-Situ measurements with specifically designed samples

From the samples that where In-Situ monitored from phase II a lot could be learned, for example of how the warm hot end temporally increases the resistance of a test-sample, even when a new layer is applied which should suppose to be lowering the measured resistance. However, From the plots used for test pieces in phase II, this phenomenon is hard to see (due to lack of pause in between the layers and the placements of the electrodes in the part), hence why a new test sample had to be created. This new sample was specifically designed for the paper mentioned in the introduction of this chapter an image of this sample can be seen in Figure 6.1

The sample did not use a perforated copper tape structure like in the samples of phase II, this because in the In-Situ monitoring paper the goal is mainly focused on investigating what effects each layer of a conductive polymer has on the total resistance of the print. To investing this layer behaviour, a pause of 5 and later 7 minutes is introduced between the printing of the layers. A schematic overview of this setup and the results of the two layers can be seen in Figure 6.2

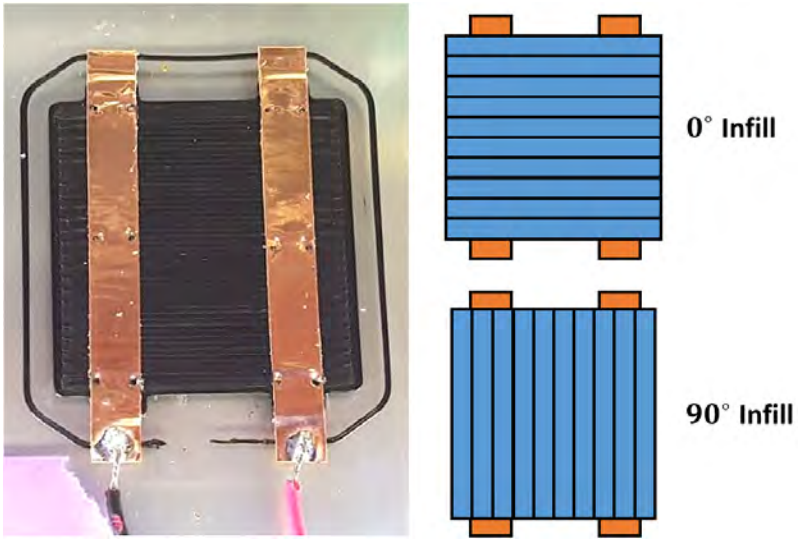

Figure 6.1: Specifically designed sample for the In-Situ monitoring paper, in this way influences regarding the infill directions of 0°and 90°, could be tested as well

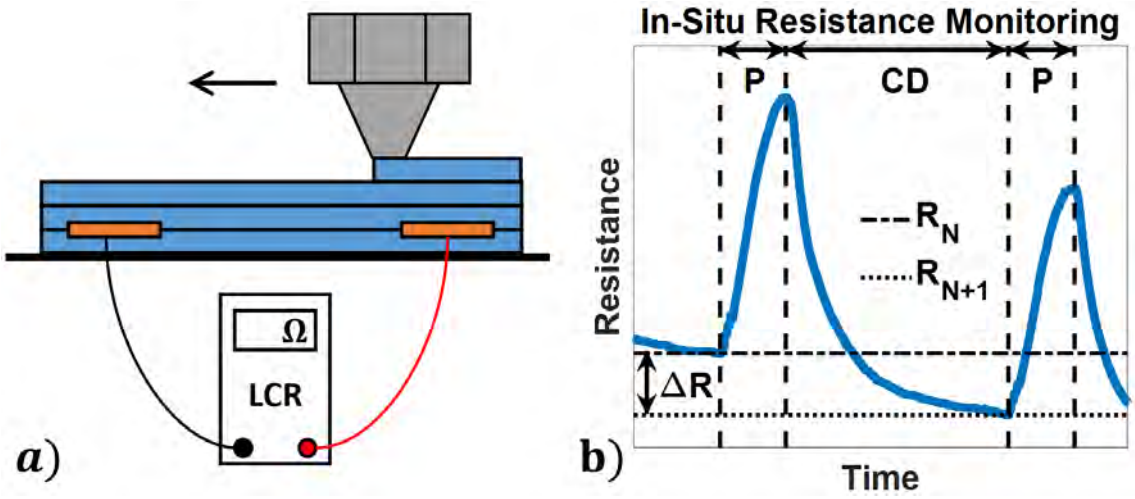

Figure 6.2: Here you can see how the nozzle moves over the print with embedded electrodes, this movement creates a peak which can be seen in the graph. After the printer goes into a pause of the mentioned 5 or 7 minutes the resistance decreases exponentially.
Note: *P stands for printing CD stands for cool down an N is the layer number*

6.3 Results

Only the results for the experiment using the designed sample from phase II will be published in this section, the reason why is that this report is about researching the contact resistance and not explicitly about In-Situ monitoring. This method was introduced to try to find a possible cause that could explain why the test samples from phase II started with such unexpectedly high resistance. The results of In-Situ monitoring 5 ETPU prints samples and 2 ProtoPasta samples were each put into a sub-figure. The plot of the two sub-figures can be seen in Figure 6.3. The results from these In-Situ monitoring were quite remarkable, the hot end moving over the sample while printing the next layer actually did let the resistance of the sample increase, this can be seen in Figure 6.3. There is a rise in resistance and then a peak, followed by a quick cool down i.e nozzle moving away from the test sample, relocating itself to start a new layer. The effect is even better seen in Figure 6.2, (b) because the results shown there actually have a 7 min pause in between printing each layer.

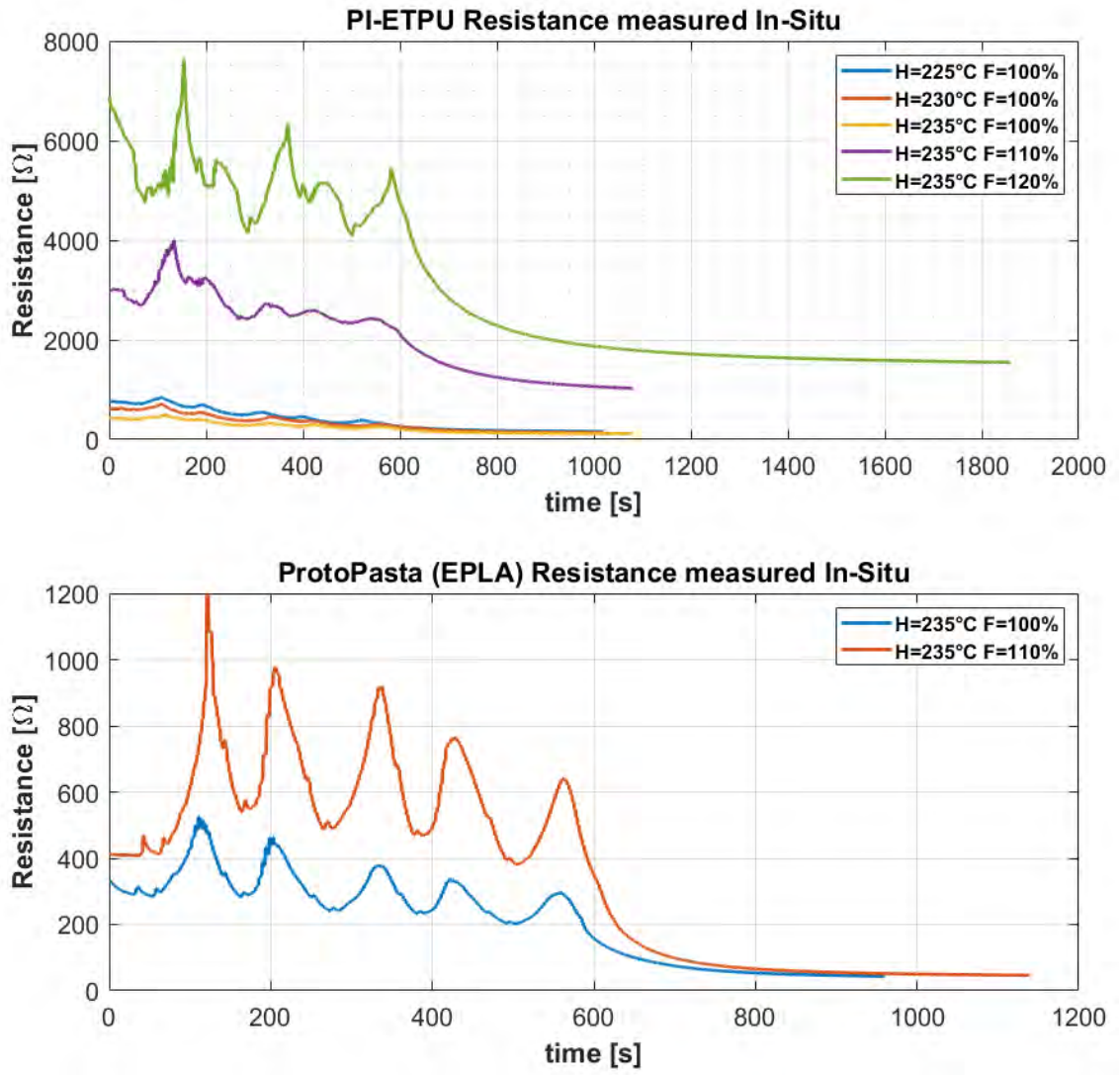

Figure 6.3: The ETPU and EPLA samples from phase II measured In-Situ without having a pause (cool down) in between the layers (Figure 6.2, (b)).
Note: *H stands for hot end, F stands for extrusion multiplier (or flow in Cura)*

Each sample printed with a higher extrusion multiplier (so 120% instead of 100%)had a higher total resistance consecutively. So e.g. a 100% multiplier gave a much lover sample resistance than a multiplier of 110%. The resistance for the PI-ETPU (ETPU) were measured up to 4 days after the In-Situ monitoring. Even after 4 days of letting the samples just rest at room temperature, still a large (and perhaps permanent) difference in resistance between the samples was measured. The results after 4 days of letting the samples rest can be seen in Table. 6.1

Table 6.1: 4 PI-ETPU samples measured after 4 days of just laying in my room, the results are ordered by printing temperature, hence why the first 3 extrusion multiplier values are the same.

MATERIAL	NOZZLE TEMP	EXTRUSION MULTIPLIER	RESISTANCE [Ω]
ETPU	225C	100%	110
ETPU	230C	100%	90
ETPU	235C	100%	88
ETPU	235C	110%	597
ETPU	235C	120%	1008

The results from 6.1 show that the best sample is created with the highest temperature of 235°C and an extrusion multiplier of 100%. No table has been made for the EPLA samples, after a couple of hours was the difference in sample resistance not significant anymore (in the range of 0-100 Ω). Furthermore, the ProtoPasta (EPLA) samples were so brittle that removing them from the glass print bed resulted in their destruction.

Another thing to mention is with the samples printed at a much higher extrusion multiplier (110%/120%) is that the surface looked like it was smeared by the nozzle, this "smearing" can be seen in the red square in Figure 6.4

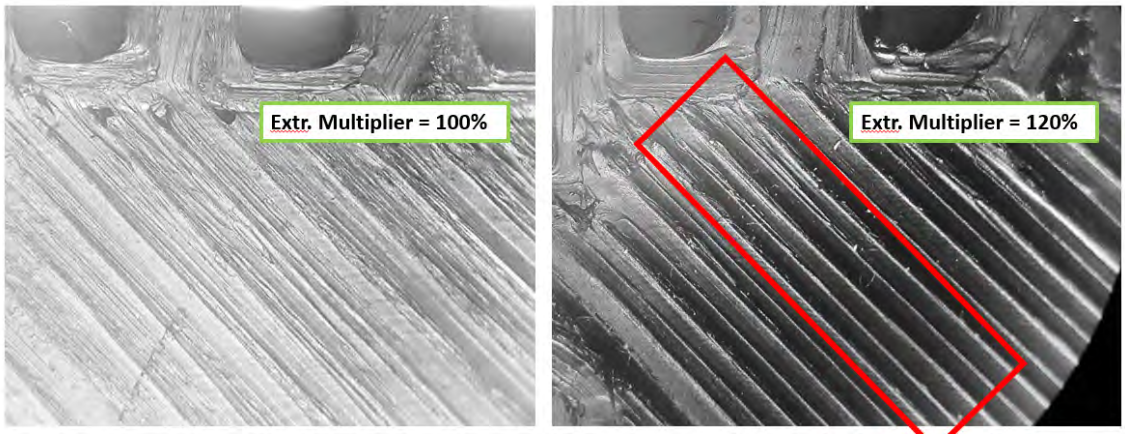

Figure 6.4: This figure shows the difference in surface finish between the best and worst samples. Both the best and worst sample are printed a temperature of 235°C at 15 mm/s and a bed set to a temperature of 65°C
Note: *the contrast of both images is boosted, to make it more clear that the sample on the right has ridges in its surface. Under my stereo microscope is this much better to see, because of the depth perspective*

6.4 Discussion and conclusion

This phase learned us a lot, e.g that the combination of nozzle temperature and extrusion multiplier can cause a seemingly permanent increase in sample resistance, and this increase doesn't have to be caused by poor electrical contact between the copper tape and the conductive polymer. The samples, that are printed with varying nozzle temperatures and varying extrusion multiplier are worth investigating further. With this novel In-Situ resistance measurement technique, it's possible to make sensors more accurately and foremost important to have a predictable resistance or impedance value.

The In-Situ resistance measurement can even be extended to a setup, where the nozzle itself can function as a (positive) measurement probe and multiple (ground) connections on the print bed and make a resistance tomography of the test sample. In this way a resistance map of a 3D-printed sensor can be made, making the complicated matter what is 3D-printing conductive sensors hopefully more predictable and understandable.

7 Over-all (Rode Draad) Conclusion and Discussion

7.1 Conclusion and Discussion of the chapters

The last chapter of this research will conclude and discuss the important findings from the previous chapters, followed by research ideas that can be executed in the future, to further complete this work. We will now walk through the chapters and conclude each of the important findings.

From the theory and literature being researched for this report, a general idea could be created of which physical properties are important for good conduction between two dissimilar materials. These properties are: having two large surfaces with a lot of asperities that can touch, and so forming a lot of (large) a-spots (current-conducting paths). The volumetric resistance ratio of the conductor and conductive polymer is important as well. Based on the ratio, will the normalised contact resistance increase or decrease. And final, with the help of the RaM sensor investigation, ballpark contact dimensions and electrical requirements can be finalised and used for phase I

From phase I is concluded that perforated copper tape with 600 µm holes is required to establish a good mechanical bond between a 3D-printed conductive polymer and a metal, even at a small scale of just 2 traxels covering the tape. Due to this perforated approach could the contact be scaled down to 6.35 by 7 or 8 millimetre, this would fit in the range of used contact sizes used in the RaM sensors investigation. Furthermore, the bed or better said the environment temperature is crucial for a good bond, ETPU traxels that were printed on a 600 µm TPU base layer at a bed temperature of 60°C were almost impossible to be peeled off, the samples did break at a material level instead, instead of breaking on a surface adhesion level.

From phase II is concluded: to have a strong mechanical bond, between a perforated metal (copper tape) and conductive polymer, an overmolding procedure needs to be used. In this process will perforated copper tape be covered in hot conductive polymer extruded by 3D-printer nozzle. It's important that during overmolding process, the temperature of the sample is at least at 60 to 65°C. For the perforation in the tape it's important to use as many 600 µm holes that will fit on the given surface since from the tests executed, the samples with the most amount of holes achieved the lowest resistance after hours of cycle testing. Furthermore, the fluctuations in measured resistance, caused by the cyclic loading and unloading are the smallest.

In my opinion, it would even be better to fix the location where the contact is housed in place. E.g. superglue the location of where the contact is printed to something stiff. In this way, the only part of the sensor that can flex is the part that is designed to be a sensor (excluding the contact islands). A small scale experiment is done with a real 3D-printed test sensor, which is shown in Figure 7.1. There is an actual test with this sensor comparing it against melting in the test-wires with a soldering iron, compared to the perforated copper tape that's being overmolded by the nozzle. The clear winner of this test was the perforated copper tape, both did well in terms of electrical conductivity. But the wire was ripped out which less force than the copper tape.
Note: *This, test is done on video so its not possible to include it in the report.*

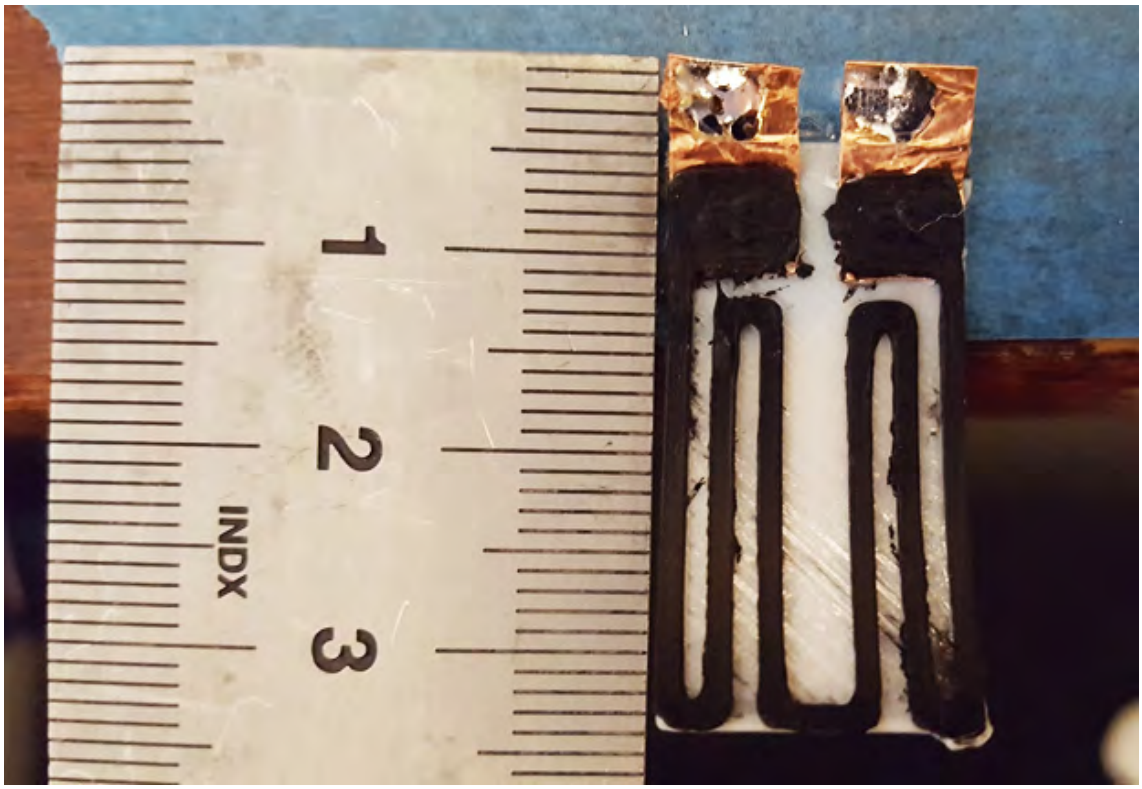

Figure 7.1: 1 mm thick (two ETPU layers) sensor, this in order to really show the capabilities of the punctured copper tape and the robustness of the mechanical interlocking though the holes. The islands of where the contacts are housed are super glued to the blue backing tape.

From Phase III is concluded that it's important to have a hot end temperature and the extrusion multiplier chosen that is suitable for the conductive polymer that is used for the experiments. For ETPU a hot end is set to 235°C and an extrusion multiplier of 100% these settings gave the lowest final sample resistance (compared to 235°C and 120%). Without In-Situ resistance monitoring (the new method introduced), would it be much harder to find those optimal temperature and extrusion multiplier settings. The printer could in theory have a feedback system that could tweak parameters like bed temperature, hot end temperature, and extrusion multiplier during the print to produce a sensor that is of a known value and even after cooling down will have the desired value. The next section will cover future research because a lot of important things have not been done in this report.

7.2 Future FDM research with conductive polymers

It would be ideal in future research, to repeat the experiments from this report but then using an AC analysis. Combining AC analysis with In-Situ Impedance monitoring or even tomography, the complex behaviour of a sensor can be studied. In this way, the bridge between printing inductive or capacitive sensors can be narrowed. In this report only two materials are used: ProtoPasta conductive PLA (EPLA) and PI-ETPU (ETPU), it would most definitely be interesting to test more and even higher conductive materials like conductive electrify filament [17]. However, this non-carbon-based polymer filament could be susceptible to oxidation. Furthermore, the nozzle used in this research was a stainless steel nozzle of 800 µm, different nozzle materials and diameters need to be tested to verify if the found result does follow the same trends with e.g different nozzles sizes. The layer height was set for the samples in phase II and III to a height of 250 µm, so for further research, investigating the effects of changing this layer-height to a smaller value would most definitely be worth to investigate. And now with the new method of doing the In-Situ resistance measurements, the results of such a layer height reduction could immediately be seen during the print process.

7.3 Recommendation for future conductive MSLA research

One last method to print better contacts and more conductive parts could perhaps be achieved by mixing a photo-polymer with conductive nanoparticles. Because during the print process an entire layer can be cured at the same time could this mean that the carbon particles are dispersed more evenly and perhaps eliminate the complex structure that FDM printing brings with conductive traxels? This method would of course need a lot of research and its something to consider for the in the further future.

A Appendix

A.1 phase I extra's (sample characterisation tables and punch images)

Here are some extra pictures shown regarding phase I

RUN	A			Date				9-6-2020		
Printer Settings				Environment						
Track Height	200		µm	Room Temp				22.6		°C
Retraction Length	0		mm	Relative Humid				41.9		%
Retraction Speed	0		mm/s	Glass Plate Temp				28.2		°C
Print Speed	5		mm/s	Silver Paint				YES	NO	
Exturder Multiplier	150		%	Probe Offset				0.2		Ω
Bed Temp	40		°C	ρ-Material				375		Ωcm
Print Temp	240		°C	Calculated Resistance				2407.33		Ω
Material	ETPU			Cleaning Copper				IPA		
Track ID	1	2	3	4	5	6	7	8	9	10
Track Width [µm]	1860	1840	1910	2100	2000	2000	1820	1840	1760	1960
Track Height [µm]	200	200	200	200	200	220	210	210	200	200
Tape Gap [µm]	250	250	250	250	250	250	250	250	250	250
Mearsured R per track[Ω]	4100	3600	1900	1800	2000	1400	2100	2300	2700	2000
Calculated R per track [Ω]	2520	2548	2454	2232	2344	2131	2453	2426	2663	2392
Average Measured	2389.8		Ω	Difference				17.5275		Ω
Remarks	After pulling up on track 5 medium force the maximum resistance reached 4100 ohm after relasing the pull the resistance fluctuated between 2000 and 4100 ohm Pulling the copper tape off wasn't to hard compared to sampe C									

RUN	C			Date				10-6-2020		
Printer Settings				Environment						
Track Height	200		µm	Room Temp				21.7		°C
Retraction Length	0		mm	Relative Humid				41.2		%
Retraction Speed	0		mm/s	Glass Plate Temp				28.3		°C
Print Speed	5		mm/s	Silver Paint				YES	NO	
Filament Flow	150		%	Probe Offset				0.2		Ω
Bed Temp	60		°C	ρ-Material				375		Ωcm
Print Temp	240		°C	Target Resistance				3669.35		Ω
Material	ETPU			Cleaning Copper				IPA		
Track ID	1	2	3	4	5	6	7	8	9	10
Track Width [µm]	1570	1720	2120	1920	1990	1890	1940	1950	1820	1769
Track Height [µm]	230	220	220	210	210	200	240	210	210	210
Tape Gap [µm]	500	400	400	400	400	400	400	400	400	250
Resistance [Ω]	2600	2000	2400	2000	2500	2300	2400	2500	3000	4000
Theroretical R per track [Ω]	5192	3964	3216	3720	3589	3968	3222	3663	3925	2524
Average Measured	2569.8		Ω	Difference				1099.55		Ω
Remarks	After pulling on track 5 the resistance went up to 3500 ohm and after relasing the pulling resistance went doewn to 2300 ohm. Pulling on the stakes almost impossible to pull off.									

Figure A.1: Some ETPU samples that were characterised into the designed data processing tables

RUN	B			Date				10-6-2020		
Printer Settings				Environment						
Track Height	200		µm	Room Temp				22.4		°C
Retraction Length	0		mm	Relative Humid				41.1		%
Retraction Speed	0		mm/s	Glass Plate Temp				28.9		°C
Print Speed	5		mm/s	Silver Paint				~~YES~~	NO	
Filament Flow	150		%	Probe Offset				0.2		Ω
Bed Temp	50		°C	ρ-Material				375		Ωcm
Print Temp	240		°C	Target Resistance				2467.35		Ω
Material	ETPU			Cleaning Copper				IPA		
Track ID	1	2	3	4	5	6	7	8	9	10
Track Width [µm]	1790	1640	1770	1770	1730	1690	1820	1950	1980	2040
Track Height [µm]	220	220	210	200	200	220	210	210	200	200
Tape Gap [µm]	250	250	250	250	250	250	250	250	250	250
Resistance [Ω]	10000	7000	4000	4500	2000	2200	1400	1800	4000	2300
Theroretical R per track [Ω]	2381	2598	2522	2648	2710	2522	2453	2289	2367	2298
Average Measured	3919.8		Ω	Difference				1452.45		Ω
Remarks	Track 8 after pulling approximatly 5kohm. When pulling on the contact, the resistace goes down. Pulling off the tracks is more difficult than @40C									

RUN	D			Date				10-6-2020		
Printer Settings				Environment						
Track Height	200		µm	Room Temp				22.1		°C
Retraction Length	0		mm	Relative Humid				45.3		%
Retraction Speed	0		mm/s	Glass Plate Temp				31.4		°C
Print Speed	5		mm/s	Silver Paint				~~YES~~	NO	
Filament Flow	150		%	Probe Offset				0.2		Ω
Bed Temp	40		°C	ρ-Material				200		Ωcm
Print Temp	260		°C	Target Resistance				2169.29		Ω
Material	ETPU			Cleaning Copper				IPA		
Track ID	1	2	3	4	5	6	7	8	9	10
Track Width [µm]	1590	1570	1900	1600	1870	1950	1950	1780	1760	1760
Track Height [µm]	210	210	190	200	220	250	210	200	190	200
Tape Gap [µm]	400	400	400	400	400	400	400	400	400	400
Resistance [Ω]	2200	1300	1500	2900	2064	1800	960	2500	2230	1465
Theroretical R per track [Ω]	2396	2426	2216	2500	1945	1641	1954	2247	2392	2273
Average Measured	1891.7		Ω	Difference				277.592		Ω
Remarks	ETPU is verry brittle and tears really easially.									

Figure A.2: Some ETPU samples that were characterised into the designed data processing tables

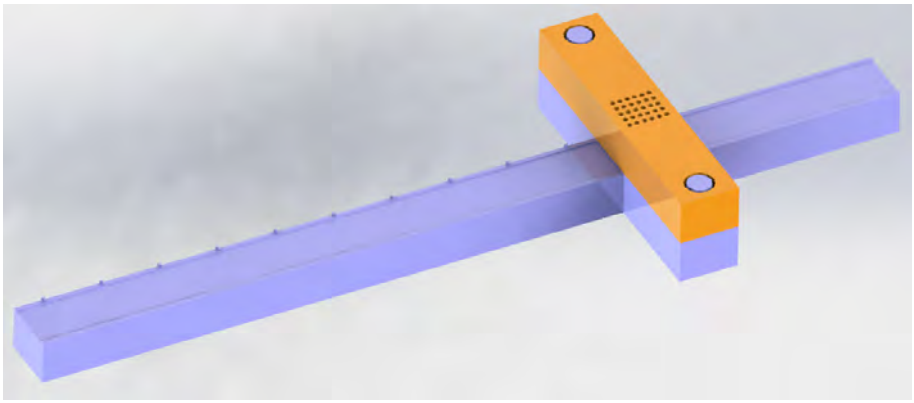

Figure A.3: CAD model of the jig in phase I, to punch precise 10 holes repeatedly with equal spacing

A.2 phase II extra's (punch images)

Here are some extra pictures shown regarding phase II

Figure A.4: CAD model of the jig in phase II used to punch the bulk of the holes and the precise holes in conductor 1

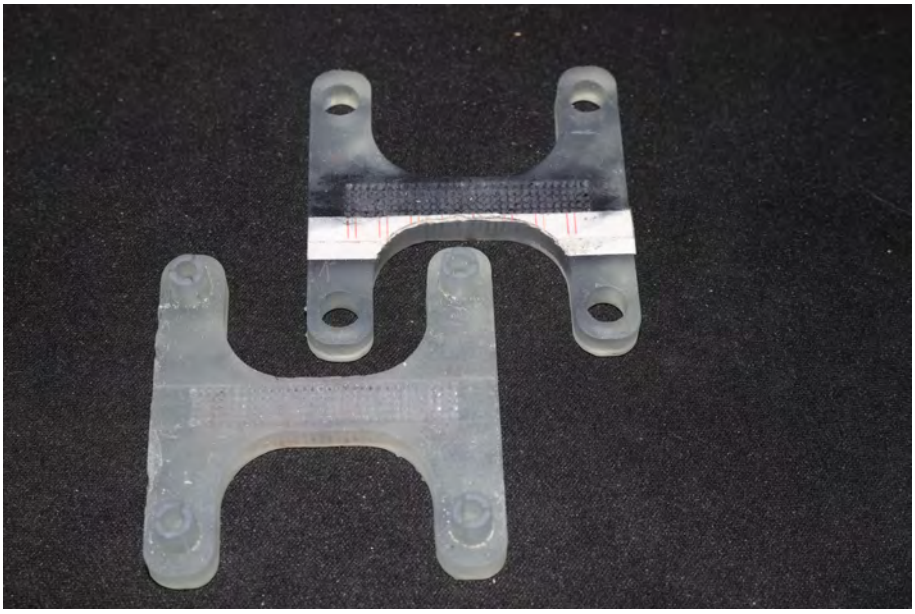

Figure A.5: Jig used to puncture holes in phase II

Figure A.6: Jig used to puncture holes in phase II in greater detail

A.3 phase III extra's (In-Situ conference paper)

Here is the conference paper added for In-Situ resistance monitoring.

In-Situ Monitoring of Layer-Wise Fabrication by Electrical Resistance Measurements in 3D Printing

Alexander Dijkshoorn, Patrick Neuvel, Stefano Stramigioli, Gijs Krijnen
Robotics and Mechatronics, University of Twente, Enschede, The Netherlands
Email: a.p.dijkshoorn@utwente.nl

***Abstract*—This paper introduces a characterization technique to study 3D-printing of conductors and sensors during fabrication. Currently characterization of 3D-printed sensors is done after fabrication. In our novel method, however, the electrical resistance is monitored in-situ by electrically contacting the part in the beginning of the print process. This way, the effect of every additional layer on the total resistance is determined. Our new experimental method opens up ways to study 3D-printing of sensors in order to better understand the processes at hand, e.g. it may allow distinguishing between bulk and inter-layer resistances. FEM simulations and experiments are used to validate the use of this new method.**

***Index Terms*—Electrical Resistance, Monitoring, 3D-Printing, Fused Deposition Modelling**

I. Introduction

3D-printing of conductors by means of Fused Deposition Modelling is a promising technique for fabrication of customisable conductors and sensors [1], [2], [3]. FDM works by means of extruding molten plastic line per line, one layer at a time. Usually conductive-polymer composites are used to obtain electrical conduction with FDM, e.g. a polymer filled with nano-particles like carbon black or carbon nanotubes [4], [5], [6]. The layer-wise fabrication process introduces anisotropic electrical properties [7], [8], by improper fusion between layers and between lines or track-elements (traxels). These anisotropic properties can affect or even improve sensor performance [9], [10]. Currently the (anisotropic) electrical properties of 3D-printed conductors and sensors are characterized after the fabrication process. This is mainly done with global resistance or impedance measurements [8], [11], although a recent study also shows Scanning Electron Microscopy and infrared thermography measurements to determine the distributed electrical properties on single layers [12] With these methods it is very difficult to distinguish the effect of the printing parameters on the electrical resistance of the individual layers in a larger print. In-situ measurements during printing can offer a solution in this respect. Several in-situ techniques already exist for quality monitoring in FDM printing. Techniques are, among others, based on optical scanning [13], computer vision [14], acoustics [15], vibrations [16], strain [17], rheological [18] and thermal measurements [19]. However, to the best of the authors knowledge an in-situ technique for monitoring the electrical properties has not yet been proposed. Therefore this paper presents the first in-situ monitoring technique of the electrical resistance in FDM. By means of inserting electrical contacts before or during printing (e.g. the electrical connections of a conductive sensor) the resistance added by every layer on top of the electrical contacts can be measured and the effects of printing parameters can be studied.

The following sections present the measurement principle and show experimental data and FEM simulations to proof the use of this technique for monitoring 3D-printing of sensors.

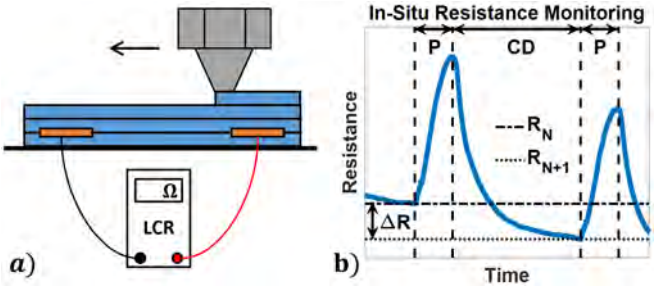

Fig. 1. **a.** Electrical contacts (e.g. used as connections to the printed sensor) are stuck onto the printing bed or embedded inside the initial layers of the 3D-print and used to monitor the electrical resistance. A 3D-printing nozzle extrudes molten plastic onto the sample layer by layer. The electrical resistance can be measured with a multi- or LCR- meter during printing. Ideally every added layer aids in lowering the electrical resistance. **b.** During printing (P) the temperature dependent resistance goes up. After printing the resistance goes down during cool down (CD). The added layer yields a lower total resistance (going from N to $N+1$ layers), which is followed by printing another layer.

II. Measurement Principles

The measurement principle is based on a basic electrical resistance measurement. Electrical contacts are fixed on the printing bed or embedded during printing to monitor the electrical resistance (and may later be used as electrical contacts for the sensor), figure 1.a. This can be used to study the changes in electrical resistance with added layers, the contact resistance between layers and the effect of printing parameters. The method can also be applied as a proxy to monitor other properties of parts that use conductive-polymer composites, for example for the mechanical, thermal or electrostatic charge dissipative nature of these materials [20]. One challenge for this measurement principle is the strong rise in electrical resistivity due to an increase in temperature (the targeted

This work was developed within the PortWings project, funded by the European Research Council, Grant Agreement No. 787675. and the Wearable Robotics programme, funded by the Dutch Research Council (NWO).

materials generally have a positive temperature coefficient, or PTC), often followed by a negative dependence of the resistivity on the temperature above the melting temperature [21]. The general accepted explanation for the PTC effect is believed to be a mismatch of thermal expansion coefficient between polymer and filler, especially at a phase transition (melting) of the polymer matrix [21]. This is encountered with FDM when the hot plastic and nozzle heat up the sample, causing the electrical resistance to increase during printing, phase P in figure 1.b. This challenge can be reduced or overcome by letting the sample cool down between printing of each layer, phase CD in figure 1.b. Hence, during printing of a layer the resistance ramps up and after printing the resistance drops exponentially.

III. Methodology

A. Experimental Set-Up

Experiments are performed with a customised Ultimaker 2 printer with a BondTec direct drive extruder, a water cooled hot end and an E3D stainless steel nozzle of 0.8 mm. Samples are designed in SolidWorks CAD software and slicing is performed with Cura. As materials a conductive carbon black filled Polylactic Acid (PLA) called Proto-Pasta [22]) and a conductive carbon black filled TPU filament called PI-ETPU 85-700+ from Palmiga Innovation [23] are used. The samples are plates of 40 mm wide by 40 mm with a layer thickness of 250 µm, where they have a different number of layers depending on the test. Copper tape of 6.35 mm wide and 66 µm thick with conductive acrylic adhesive is used as electrical contacts. Alignment tabs are printed on the side of the sample to place two pieces of copper tape consistently at a distance of 16 mm, figure 2.a. The tape is added after printing two layers of material for reliable embedding. 6 small holes are punched in the tape and touched with a soldering iron at 400 °C to prevent the printer pushing the tape away when printing. During the tests the print bed is kept at 50 °C, whereas the nozzle is kept at 230 °C. The fan is not used to reduce cooling below the print bed temperature. A single infill angle is used per sample, of either 0° or 90° as shown in figure 2.a. The extrusion multiplier (or flow rate) is taken at 100 % or 110 %. Electrical resistance measurements are performed with the DC mode of an LCR (UNI-T UT612 LCR Meter). After printing each layer, the printer is paused for 5 minutes to let the sample cool down before printing the next layer.

B. FEM Simulations

In order to test our understanding of the measurement method, FEM simulations are performed. The structures are simulated in 2D using the Electric Currents module in COMSOL. A 2D simulation can be used since the sample has a uniform cross section. A voltage terminal and a ground are included to represent the copper electrical contacts over which the resistance is measured. Resistance between the printed layers is implemented through the contact impedance functionality. A parameter sweep is performed over the number of layers (ranging from 2 to 12, where the electrical contacts are placed on top of the second layer), for resistivity (ρ) values of 0.15 Ω m and 0.25 Ω m, and for isotropic conditions (a sample without inter-layer resistance) and an inter-layer contact resistance (σ) of 1×10^{-2} Ω m^2.

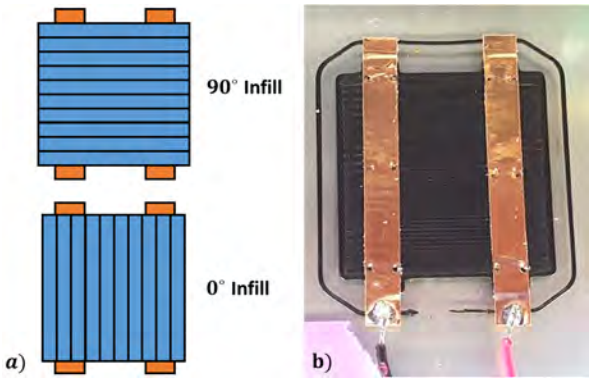

Fig. 2. **a.** The tow infill angles used in the experiments: printing parallel (0°) and perpendicular (90°) to the electrical contacts. **b.** The first two layers of a sample with electrical contacts added on top of it. Six holes are punctured in each electrical contact and touched with a soldering iron to keep it in place during printing.

IV. Results

The first two layers of a sample with the copper contacts are shown in figure 2.b. The infill in this sample is 90°, yielding traxels perpendicular to the electrical contacts. The resistance measurement is started directly following the application of the electrical contacts.

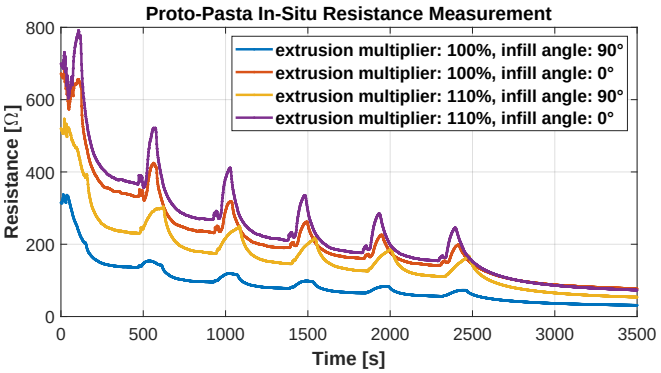

Fig. 3. Resistance over time for various print settings (extrusion multiplier, infill pattern) for conductive PLA. The peaks arise from heating during printing and subsequent cooling down after printing.

Figure 3 shows measurements for various Proto-Pasta samples, whereas figure 4 shows the same measurements for ETPU samples. The start of the print of successive layers can be identified from the periodic peaks. Furthermore it becomes clear that every added layer lowers the total resistance. The resistance starts high and drops before the first layer is printed, since adding the electrical contacts with the soldering iron heats up the material significantly. Next to that the measurements show that an extrusion multiplier of 100% yields a lower

resistance than 110% and an infill angle of 90° yields a lower resistance than 0° for both materials (even after several days). Moreover for infill angles of 90° the peak of the first layer is very small compared to the other peaks. Finally the peaks for 0° are always sharper and more pronounced than for 90°.

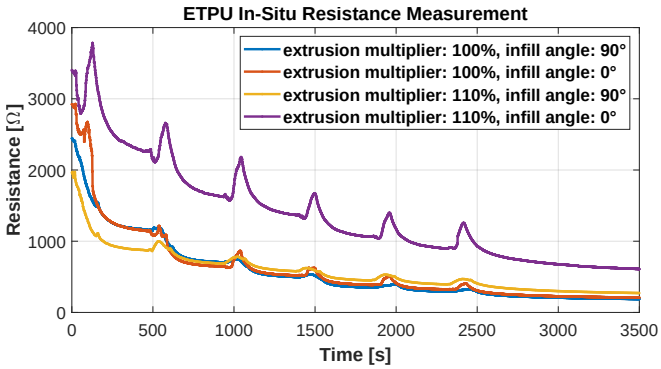

Fig. 4. As Figure 3 but results are for conductive TPU.

Additional measurements are performed on a Proto-Pasta sample composed of 12 layers for comparison with the FEM simulations. It is fabricated with an extrusion multiplier of 100%, an infill angle of 0°, an increased cool down period of 7 minutes and copper contacts on top of the second layer. Figure 5 compares the measured total resistance versus the number of layers with the corresponding FEM simulations for an isotropic model and for a model with high inter-layer resistance of $1 \times 10^{-2}\,\Omega\,\mathrm{m}^2$. For the simulations with high inter-layer resistance it becomes clear that the total resistance barely changes going from 10 to 12 layers. On the other hand for the isotropic simulation, adding material in this range still significantly lowers the total resistance. The experimental curve lies somewhere in between these two scenarios, indicating the presence of inter-layer resistance. The FEM simulations do not take into account contact resistance and parasitic resistance of the set-up. For low numbers of layers the measurements and simulations do not fit well.

V. Discussion and Conclusions

The proposed novel measurement method clearly shows the change in resistance per printed layer. The measurements show strong qualitative similarity for different print settings and materials, enabling an easy comparison of results. Resistance (changes) during measurements are highly correlated with the resistances after cooling down, allowing for optimisation of electrical conductivity in 3D printed conductors and sensors. Since the method uses embedded electrical contacts, these can be used after fabrication as connections to the sensors, and vice versa sensor connections can already be used during fabrication for monitoring.

Several remarks can be made about the results. The measurement results show an interesting difference in height and sharpness of the resistance peak for the two different infill angles in figures 3 and 4. This can likely be explained from the temperature dependence of the resistivity in combination

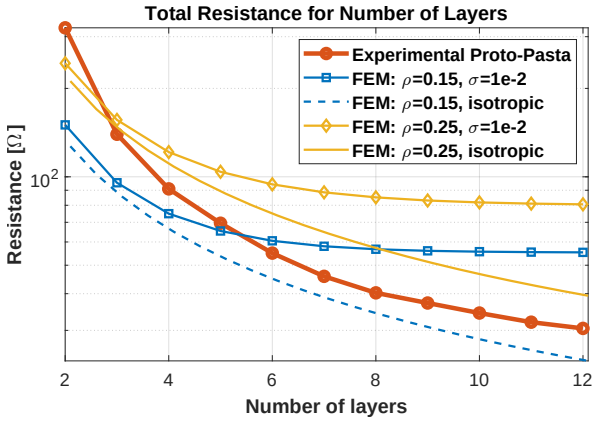

Fig. 5. The total measured resistance compared to FEM simulation results as a function of number of layers. FEM simulations are performed for isotropic conditions (a single material without layers), and high inter-layer resistance of $1 \times 10^{-2}\,\Omega\,\mathrm{m}^2$.

with the infill angle. For an angle of 0° the nozzle heats up the sample in parallel to the electrodes, so the current always flows through a just heated section with a high resistivity. For 90° the nozzle heats up the sample perpendicular to the electrodes, so the current can always flow through sections that have not been heated yet or have already started cooling. In this way the change in resistance over time is more pronounced for an infill angle of 0°. Another remark is that the measurements and FEM simulations do not fit well for small numbers of layers. One explanation for this could be a poor connection between the electrical contacts and the print at the start, giving a high contact resistance. When the first layers are printed on top of the contacts, the nozzle then pushes on them, melts the plastic and in this way lowers the contact resistance. This would be an explanation for the measured high resistance at low numbers of layers. Furthermore the method currently has two major challenges. A first challenge for the new method is the placement of the electrical contacts. Only after placing the contacts one can start measuring. Therefore contacts have to be on the print bed or in the first layers to monitor the resistance for the largest part of the fabrication process. A second challenge for the new method is posed by the thermal effects. Cooling down of the sample in between printing helps to get a more reliable resistance measurement. However, it is still unclear how the inhomogeneous heating from the bed heating below and the nozzle above influences the resistivity throughout the sample and if cooling down is sufficient. This challenge could be reduced significantly by heating the entire environment around the sample up to the bed temperature.

Future research is aimed at gaining more understanding of the method. A next step will be studying the use of the method for different print parameters as well as electrode and print geometries to see how it can be used for optimisation of 3D-printed electrical conductive structures. Finally it can be researched if the optimised parameters obtained by studying fusion in conductive materials can also be used for improving regular mechanical prints.

REFERENCES

[1] A. Dijkshoorn, P. Werkman, M. Welleweerd, G. Wolterink, B. Eijking, J. Delamare, R. Sanders, and G. J. Krijnen, "Embedded sensing: Integrating sensors in 3-D printed structures," *Journal of Sensors and Sensor Systems*, vol. 7, no. 1, pp. 169–181, 2018.

[2] Y. Xu, X. Wu, X. Guo, B. Kong, M. Zhang, X. Qian, S. Mi, and W. Sun, "The boom in 3d-printed sensor technology," in *Sensors (Basel, Switzerland)*, 2017, pp. 1–37.

[3] M. R. Khosravani and T. Reinicke, "3D-printed sensors: Current progress and future challenges," *Sensors and Actuators, A: Physical*, vol. 305, p. 111916, 2020. [Online]. Available: https://doi.org/10.1016/j.sna.2020.111916

[4] S. W. Kwok, K. H. H. Goh, Z. D. Tan, S. T. M. Tan, W. W. Tjiu, J. Y. Soh, Z. J. G. Ng, Y. Z. Chan, H. K. Hui, and K. E. J. Goh, "Electrically conductive filament for 3D-printed circuits and sensors," *Applied Materials Today*, vol. 9, pp. 167–175, 2017.

[5] P. F. Flowers, C. Reyes, S. Ye, M. J. Kim, and B. J. Wiley, "3d printing electronic components and circuits with conductive thermoplastic filament," *Additive Manufacturing*, vol. 18, pp. 156 – 163, 2017.

[6] A. Joshi, J. K. Goh, and K. E. J. Goh, "Chapter 3 - polymer-based conductive composites for 3d and 4d printing of electrical circuits," in *3D and 4D Printing of Polymer Nanocomposite Materials*, K. K. Sadasivuni, K. Deshmukh, and M. A. Almaadeed, Eds. Elsevier, 2020, pp. 45 – 83.

[7] B. Hampel, S. Monshausen, and M. Schilling, "Properties and applications of electrically conductive thermoplastics for additive manufacturing of sensors," *Technisches Messen*, vol. 84, no. 9, pp. 593–599, 2017.

[8] J. Zhang, B. Yang, F. Fu, F. You, X. Dong, and M. Dai, "Resistivity and Its Anisotropy Characterization of 3D-Printed Acrylonitrile Butadiene Styrene Copolymer (ABS)/Carbon Black (CB) Composites," *Applied Sciences*, vol. 7, no. 1, p. 20, 2017.

[9] G. Wolterink, R. Sanders, and G. Krijnen, "Thin, Flexible, Capacitive Force Sensors Based on Anisotropy in 3D-Printed Structures," *Proceedings of IEEE Sensors*, vol. 2018-Octob, pp. 2–5, 2018.

[10] S. Mousavi, D. Howard, F. Zhang, J. Leng, and C. H. Wang, "Direct 3d printing of highly anisotropic, flexible, constriction-resistive sensors for multidirectional proprioception in soft robots," *ACS Applied Materials & Interfaces*, 2020, pMID: 32129594.

[11] H. Watschke, K. Hilbig, and T. Vietor, "Design and characterization of electrically conductive structures additively manufactured by material extrusion," *Applied Sciences (Switzerland)*, vol. 9, no. 4, pp. 1–25, 2019.

[12] A. Dijkshoorn, M. Schouten, G. Wolterink, R. Sanders, S. Stramigioli, and G. Krijnen, "Characterizing the electrical properties of anisotropic, 3d-printed conductive sheets for sensor applications," *accepted in IEEE Sensors*.

[13] L. Li, R. McGuan, P. Kavehpour, and R. Candler, "Precision enhancement of 3d printing via in situ metrology," 2020, pp. 251–260.

[14] C. Liu, A. C. C. Law, D. Roberson, and Z. J. Kong, "Image analysis-based closed loop quality control for additive manufacturing with fused filament fabrication," *Journal of Manufacturing Systems*, vol. 51, pp. 75 – 86, 2019.

[15] H. Wu, Y. Wang, and Z. Yu, "In situ monitoring of fdm machine condition via acoustic emission," *International Journal of Advanced Manufacturing Technology*, vol. 84, no. 5-8, pp. 1483–1495, 2016, cited By 43.

[16] Y. Li, W. Zhao, Q. Li, T. Wang, and G. Wang, "In-situ monitoring and diagnosing for fused filament fabrication process based on vibration sensors," *Sensors (Switzerland)*, vol. 19, no. 11, 2019.

[17] C. Kousiatza and D. Karalekas, "In-situ monitoring of strain and temperature distributions during fused deposition modeling process," *Materials and Design*, vol. 97, pp. 400–406, 2016.

[18] T. J. Coogan and D. O. Kazmer, "In-line rheological monitoring of fused deposition modeling," *Journal of Rheology*, vol. 63, no. 1, pp. 141–155, 2019.

[19] E. Ferraris, J. Zhang, and B. V. Hooreweder], "Thermography based in-process monitoring of fused filament fabrication of polymeric parts," *CIRP Annals*, vol. 68, no. 1, pp. 213 – 216, 2019.

[20] S. F. A. Acquah, B. E. Leonhardt, M. S. Nowotarski, J. M. Magi, K. A. Chambliss, T. E. S. Venzel, S. D. Delekar, and L. A. Al-Hariri, "Carbon nanotubes and graphene as additives in 3d printing," in *Carbon Nanotubes*, M. R. Berber and I. H. Hafez, Eds. Rijeka: IntechOpen, 2016, ch. 8.

[21] Y. Liu, H. Zhang, H. Porwal, J. Busfield, T. Peijs, and E. Bilotti, "Pyroresistivity in conductive polymer composites: a perspective on recent advances and new applications," *Polymer International*, vol. 68, no. 3, pp. 299–305, 2019.

[22] ProtoPlant, makers of Proto-pasta. Composite PLA - Electrically Conductive Graphite. Accessed: 31-01-2017. [Online]. Available: https://www.proto-pasta.com/

[23] Palmiga Innovation. Material info for PI-ETPU 95-250 Carbon Black the conductive and flexible 3D printing filament. Accessed: 05-03-2019. [Online]. Available: http://rubber3dprinting.com/pi-etpu-95-250-carbon-black

Bibliography

[1] A. Dijkshoorn, M. Schouten, G. Wolterink, R. Sanders, S. Stramigioli, and G. Krijnen, "Characterizing the electrical properties of anisotropic, 3d-printed conductive sheets for sensor applications," *IEEE Sensors Journal*, pp. 1–1, 2020.

[2] https://www.ram.eemcs.utwente.nl/. [accessed on: 25-06-2020].

[3] B. Eijking, "Tactile whisker sensor using flexible 3d printed transducers," July 2017.

[4] B. Prakken, "3d printed flow sensor," March 2019.

[5] H. Watschke, K. Hilbig, and T. Vietor, "Design and characterization of electrically conductive structures additively manufactured by material extrusion," *Applied Sciences*, vol. 9, no. 4, p. 779, 2019.

[6] C. Zhai, D. Hanaor, G. Proust, L. Brassart, and Y. Gan, "Interfacial electro-mechanical behaviour at rough surfaces," *Extreme Mechanics Letters*, vol. 9, pp. 422–429, 2016.

[7] P. Zhang and Y. Lau, "Scaling laws for electrical contact resistance with dissimilar materials," *Journal of Applied Physics*, vol. 108, no. 4, p. 044914, 2010.

[8] P. Zhang, Y. Lau, and R. S. Timsit, "Spreading resistance of a contact spot on a thin film," in *2013 IEEE 59th Holm Conference on Electrical Contacts (Holm 2013)*, pp. 1–7, IEEE, 2013.

[9] L. Rossing, R. B. Scharff, B. Chömpff, C. C. Wang, and E. L. Doubrovski, "Bonding between silicones and thermoplastics using 3d printed mechanical interlocking," *Materials & Design*, vol. 186, p. 108254, 2020.

[10] H. Wang, I. Bernardeschi, and L. Beccai, "Developing reliable foam sensors with novel electrodes," in *2019 IEEE SENSORS*, pp. 1–4, IEEE, 2019.

[11] https://ultimaker.com/software/ultimaker-cura/. [accessed on: 04-08-2020].

[12] Palmiga Innovation, "Material info for PI-ETPU 95-250 Carbon Black the conductive and flexible 3D printing filament." Accessed: 25-06-2020.

[13] ProtoPlant, makers of Proto-pasta, "Composite PLA - Electrically Conductive Graphite." Accessed: 25-06-2020.

[14] https://nl.farnell.com/3m/1181-6mm/tape-copper-foil-16-5m-x-6mm/dp/1653451. [accessed on: 04-08-2020].

[15] https://nl.pinterest.com/pin/550494754422121159/. [accessed on: 04-08-2020].

[16] A. Dijkshoorn, P. Neuvel, S. Stramigioli, and G. Krijgen, "In-situ monitoring of layer-wise fabrication byelectrical resistance measurements in 3d printing," 2020.

[17] https://www.multi3dllc.com/product/electrifi/. [accessed on: 5-8-2020].